[41] Teshima S, Shimosato Y, Hirohashi S, Tome Y, Hayashi I, Kanazawa H, Kakizoe T. Four new human germ cell tumor cell lines. Lab Invest 1988;59:328–36.

[42] Zeuthen J, Nørgaard JO, Avner P, Fellous M, Wartiovaara J, Vaheri A, Rosén A, Giovanella BC. Characterization of a human ovarian teratocarcinoma-derived cell line. Int J Cancer 1980;25: 19–32.

[43] Kohler PO, Bridson WE. Isolation of hormone-producing clonal lines of human choriocarcinoma. J Clin Endocrinol Metab 1971;32: 683–7.

Mutation Research 664 (2009) 20–27

Contents lists available at ScienceDirect

Mutation Research/Fundamental and Molecular Mechanisms of Mutagenesis

journal homepage: www.elsevier.com/locate/molmut
Community address: www.elsevier.com/locate/mutres

Role of Parp-1 in suppressing spontaneous deletion mutation in the liver and brain of mice at adolescence and advanced age

Atsushi Shibata[a,b,c], Daisuke Maeda[a,b], Hideki Ogino[a,b], Masahiro Tsutsumi[d], Takehiko Nohmi[e], Hitoshi Nakagama[a], Takashi Sugimura[a], Hirobumi Teraoka[c], Mitsuko Masutani[a,b,*]

[a] Biochemistry Division, National Cancer Center Research Institute, Chuo-ku, Tokyo 104-0045, Japan
[b] ADP-ribosylation in Oncology Project, National Cancer Center Research Institute, Chuo-ku, Tokyo 104-0045, Japan
[c] Medical Research Institute, Tokyo Medical and Dental University, Chiyoda-ku, Tokyo 101-0062, Japan
[d] Pathology, Saiseikai Chuwa Hospital, Sakurai-City, Nara 633-0054, Japan
[e] Division of Genetics and Mutagenesis, National Institute of Health Sciences, Setagaya-ku, Tokyo 158-8501, Japan

ARTICLE INFO

Article history:
Received 16 August 2008
Received in revised form 30 January 2009
Accepted 4 February 2009
Available online 14 February 2009

Keywords:
Parp-1
Mutation
Deletion
gpt delta
Aging

ABSTRACT

Poly(ADP-ribose) polymerase-1 knockout (*Parp-1*$^{-/-}$) mice show increased frequency of spontaneous liver tumors compared to wild-type mice after aging. To understand the impact of *Parp-1* deficiency on mutations during aging, in this study, we analyzed spontaneous mutations in *Parp-1*$^{-/-}$ aged mice. *Parp-1*$^{-/-}$ mice showed tendencies of higher mutation frequencies of the *red/gam* genes at 18 months of age, compared to *Parp-1*$^{+/+}$ mice, in the liver and brain. Complex-type deletions, accompanying small insertion were observed only in *Parp-1*$^{-/-}$ mice in the liver and brain. Further analysis in the liver showed that the frequency of single base deletion mutations at non-repeat or short repeat sequences was 5.8-fold higher in *Parp-1*$^{-/-}$ than in *Parp-1*$^{+/+}$ mice ($p < 0.05$). A 3.2-fold higher tendency of the deletion frequency of two bases or more was observed in *Parp-1*$^{-/-}$ mice compared to *Parp-1*$^{+/+}$ mice ($p = 0.084$). These results support the model that *Parp-1* is involved in suppressing imprecise repair of endogenous DNA damage leading to deletion mutation during aging. The mutation frequencies of the *gpt* gene in the brain were found to be 3-fold lower in *Parp-1*$^{-/-}$ than in *Parp-1*$^{+/+}$ mice at 4 months of age ($p < 0.01$), implying that Parp-1 may be positively involved in imprecise DNA repair in the brain. On the other hand, the frequencies of *gpt* mutation showed an increase at 18 months of age in the *Parp-1*$^{-/-}$ ($p < 0.05$) but not in *Parp-1*$^{+/+}$ brains, suggesting that *Parp-1* deficiency causes an increase of point mutations in the brain by aging.

1. Introduction

Poly(ADP-ribose) polymerase-1 (Parp-1) facilitates DNA strand break repair by binding to the end of DNA strand breaks and catalyzing transfer of ADP-ribose residues from NAD to itself and other nuclear proteins, including XRCC1 (X-ray cross-complementing factor 1) [1], WRN (Werner's syndrome protein) [2,3] and Ku70/80 [4,5]. PolyADP-ribosylation results in recruitment of DNA repair proteins to DNA damage sites [6,7]. Accumulating studies have indicated that Parp-1 is involved in base excision repair (BER) and single strand break (SSB) repair by interacting with XRCC1 through poly(ADP-ribose) residues, as well as DNA polymerase β [8] and DNA ligase IIIα [9] using the BRCT domain in Parp-1. We previously demonstrated that *Parp-1*$^{-/-}$ mice show higher susceptibility to carcinogenesis induced by alkylating agents such as *N*-nitrosobis(2-hydroxypropyl)amine (BHP) [10] and azoxymethane [11] but not with 4-nitroquinoline 1-oxide [12]. *Parp-1*$^{-/-}$ mice develop normally, and spontaneous tumor incidences in all organs are not elevated at least until 9 months old [11]. However, the incidences of hepatocellular adenomas and carcinomas in *Parp-1*$^{-/-}$ mice are increased at 18–24 months old compared to *Parp-1*$^{+/+}$ mice [13]. *Parp-1*$^{-/-}$*p53*$^{-/-}$ mice also show spontaneous medulloblastomas in *p53* knockout (*p53*$^{-/-}$) mice at a higher incidence compared to *Parp-1*$^{+/+}$*p53*$^{-/-}$ mice [14,15].

In wild-type mice, age-related increases of mutant frequencies are observed in the liver, spleen, heart and small intestine, whereas mutant frequencies in the brain and germ cells are only slightly increased [16–18]. Age-related increases in genome rearrangement as well as point mutations are reported in the liver but not observed in the brain [19]. Therefore, the effects of aging on spontaneous mutation frequency might be different among tissues.

To analyze the impact of aging on spontaneous mutant frequency and its spectra in *Parp-1*$^{-/-}$ mice, we performed mutation analysis in *Parp-1*$^{-/-}$ mice at advanced age using progeny of

* Corresponding author at: Biochemistry Division, National Cancer Center Research Institute, 5-1-1, Chuo-ku, Tokyo 104-0045, Japan. Tel.: +81 3 3542 2511; fax: +81 3 3542 2530.
E-mail address: mmasutan@ncc.go.jp (M. Masutani).

0027-5107/$ – see front matter © 2009 Elsevier B.V. All rights reserved.
doi:10.1016/j.mrfmmm.2009.02.001

intercross with *gpt* delta transgenic mice harboring about 80 copies of tandemly integrated lambda EG10 DNA as a transgene [20,21]. The rescued phage was analyzed by the Spi$^-$ (sensitive to P2 interference) assay, which preferentially detects deletion mutations in the *red/gam* genes. The deletion mutations of a single base to approximately 10 kb or several copies of EG10 DNA could be detected. The *gpt* assay detects point mutations in the guanine phosphoribosyl transferase (*gpt*) gene. The spontaneous mutant frequency of the *gpt* gene in the liver of mice is around $2–6 \times 10^{-6}$ [23] in tissues including the liver and brain [24]. The frequency of mutation in the *red/gam* genes in the liver of mice is also reported to be around $1–5 \times 10^{-6}$ [23,24].

Analysis of deletion mutation with a Spi$^-$ assay using *gpt* delta transgenic mice has been shown to be useful in detecting deletion mutations after treatment with various types of chemicals or irradiation with γ-rays or heavy ions [23,25–26].

The results in this study suggest that Parp-1 suppresses spontaneous deletion mutations, especially at non-repeat or short repeat sequences in the liver and brain during aging. Complex-type deletions accompanying small insertion and microhomology at deletion junctions observed in *Parp-1*$^{-/-}$ livers and brains are also discussed. Additionally, we observed that the mutant frequencies of the *gpt* gene in the brains were found to be 3-fold lower in *Parp-1*$^{-/-}$ than in *Parp-1*$^{+/+}$ mice at 4 months of age but increased in *Parp-1*$^{-/-}$ mice to the level of *Parp-1*$^{+/+}$ mice at 18 months of age.

2. Materials and methods

2.1. Genomic DNA extraction and rescue of the transgene

Parp-1$^{-/-}$*/gpt* delta and *Parp-1*$^{+/+}$*/gpt* delta animals were previously established by intercrossing *Parp-1*$^{+/-}$*/gpt* delta mice [20]. The mice possess mixed genetic background of C57BL/6, ICR and 129Sv. Male *Parp-1*$^{-/-}$ and *Parp-1*$^{+/+}$ mice were fed a basal diet (CE-2, Clea Japan), and these mice were anaesthetized and sacrificed at the ages of 4 months ($n = 5$ for each genotype) and 18 months ($n = 6$ (*Parp-1*$^{-/-}$) and $n = 4$ (*Parp-1*$^{+/+}$)). The livers and brains were immediately frozen in liquid nitrogen, and stored at −80 °C until DNA extraction. Genomic DNA was extracted by a RecoverEase DNA isolation kit (Stratagene). Two out of six *Parp-1*$^{-/-}$ mice (mouse ID, G60 and G94) of 18 months of age harbored tumors in the liver, and genomic DNA was extracted from areas containing no tumors. A lambda phage *in vitro* packaging reaction was performed with Transpack Packaging Extract (Stratagene). Part of the tissues were also fixed with formalin solution, routinely processed and sections were stained with hematoxyline-eosine. The experimental protocol was approved by the Ethics Review Committee for Animal Experimentation of the National Cancer Center Research Institute.

2.2. Spi$^-$ assay

A Spi$^-$ assay [21] was carried out with a modification as described previously [27]. The frequencies of background mutants were less than 10^{-8} in the Spi$^-$ assay and were negligible [28]. The data for Spi$^-$ mutant frequencies were therefore presented without subtracting the background mutant frequencies. To narrow down the deleted region, the structure of each mutation was analyzed by a Southern blot hybridization method that uses oligonucleotide DNA probes [29]. DNA sequencing of the mutated region was performed with a CEQ™ DTCS Quick Start Kit (Beckman Coulter).

2.3. gpt assay

The *gpt* assay was performed as described previously [21]. Briefly, the phages rescued from genomic DNA were transfected into *E. coli* YG6020 expressing Cre recombinase. Infected cells were cultured at 37 °C on plates containing chloramphenicol (Cm) and 6-thioguanine (6-TG) for 3 days until 6-TG resistant colonies appeared. To confirm the 6-TG resistant phenotype, colonies were restreaked on plates containing Cm and 6-TG. A 739 bp DNA fragment encompassing the *gpt* gene was amplified by PCR [30]. DNA sequencing of the target 456 bp in the *gpt* gene was performed with a CEQ™ DTCS Quick Start Kit (Beckman Coulter).

2.4. Statistical analysis

The statistical significance of differences in mutant or mutation frequencies between the two groups was analyzed by using the Mann–Whitney *U* test. When *p* value is less than 0.05, the difference was considered significant. Because the individual differences in mutant frequency became larger at advanced ages, "tendency of ≥1.5 fold increase or reduction" in the mutant frequency is also mentioned with *p* value in the text, when *p* value is equal to or larger than 0.05.

3. Results

3.1. Analysis of spontaneous mutant frequency of the red/gam genes and the gpt genes in the livers of Parp-1$^{-/-}$ mice at 4 and 18 months of age

There was no difference in the mutant frequencies of the *red/gam* genes in the liver between *Parp-1*$^{-/-}$ and *Parp-1*$^{+/+}$ mice at 4 months of age. The liver of *Parp-1*$^{-/-}$ mice at 18 months of age showed a 1.7-fold higher tendency of the *red/gam* mutant frequencies than those in *Parp-1*$^{+/+}$ mice ($p = 0.34$, Fig. 1A). The tendency of age-dependent 1.5-fold increase in mutant frequency was observed in *Parp-1*$^{-/-}$ but not in *Parp-1*$^{+/+}$ mice.

On the other hand, in the case of the *gpt* gene (Fig. 1B), in which point mutations are mostly detected, the mutant frequencies in *Parp-1*$^{+/+}$ mice showed a higher elevation at 18 months than that at 4 months ($p = 0.037$). In *Parp-1*$^{-/-}$ mice, a tendency of higher mutant frequency was noticed at 18 months compared to that at 4 months ($p = 0.14$). There was no significant difference in the mutant frequency of *gpt* gene between *Parp-1*$^{-/-}$ and *Parp-1*$^{+/+}$ mice at either 4 or 18 months (Fig. 1B).

3.2. Structural analysis of deletion mutations in the red/gam genes of Parp-1$^{-/-}$ mice at 18 months of age

The mutations in the *red/gam* genes could be categorized into deletion, base substitution and single base insertion. As shown in Fig. 1C, deletion mutation frequencies in the liver of *Parp-1*$^{-/-}$ mice showed a tendency of 1.7-fold increase compared to those in *Parp-1*$^{+/+}$ mice ($p = 0.20$). The deletion mutations could be classified into single base deletion and deletion of two bases or more (Fig. 1C). Fig. 1D shows the distribution of single base deletions of the *gam* gene in the liver of *Parp-1*$^{-/-}$ and *Parp-1*$^{+/+}$ mice at 18 months of age. Single nucleotide repeats, –AAAAA– at 227–231, –AAAAAA– at 295–300 and –GGGG– at 286–289, are known as hot spots of single base deletions in the *gam* gene of wild-type mice [28]. The frequency of single base deletions at hot spots, namely at 4–6 bp mononucleotide repeats was not increased in *Parp-1*$^{-/-}$ mice compared to *Parp-1*$^{+/+}$ mice (Fig. 1C). In contrast, the frequency of single base deletions at non-repeat sequences or short repeats of 2–3 bp mononucleotides showed a 5.8-fold increase in *Parp-1*$^{-/-}$ mice ($p = 0.031$, Fig. 1C). The single base deletions at non-repeat sequences were only observed in *Parp-1*$^{-/-}$ mice at a frequency of 4.3×10^{-7} and showed a higher frequency than that in *Parp-1*$^{+/+}$ mice ($p = 0.023$). The specific deletion mutation frequencies of two bases or more in the liver showed a 3.2-fold (Fig. 1C) higher tendency in *Parp-1*$^{-/-}$ mice than those in *Parp-1*$^{+/+}$ mice, although there was no statistical significance ($p = 0.084$). Deletions of both 2 bp–1 kb and deletions larger than 1 kb were observed in the liver of *Parp-1*$^{-/-}$ mice, whereas all three mutants in *Parp-1*$^{+/+}$ mice (Table 1) had deletions larger than 1 kb (data not shown).

The deletion mutations of two bases or more were also categorized into those that occurred at non-repeat and short repeat sequences of mononucleotides. Frequencies of deletion mutations of two bases or more at non-repeat and short repeats of mononucleotides showed a higher tendency in *Parp-1*$^{-/-}$ than *Parp-1*$^{+/+}$ mice ($p = 0.28$) at 18 months old (Fig. 1C). There was no deletion mutation of two bases or more that occurred on a mononucleotide repeat larger than 4 bp in both genotypes.

We further categorized deletion mutations of two bases or more into simple or complex types (Table 1). Complex-type deletions were defined as accompanying small insertions or recombination with deletions [20]. Complex-type deletions were found in

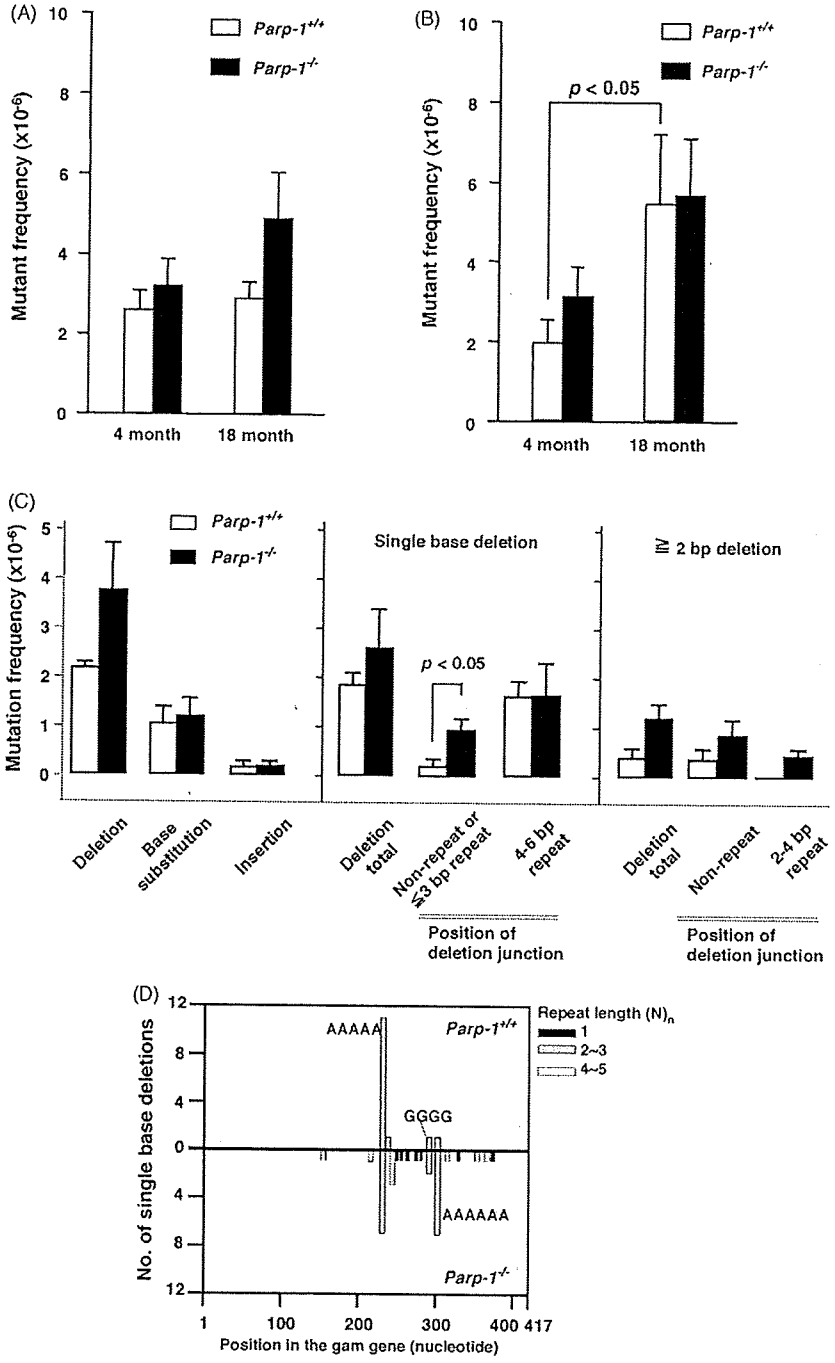

Fig. 1. Spontaneous mutant frequencies of the *red/gam* and *gpt* genes in the liver of *Parp-1*$^{-/-}$ and *Parp-1*$^{+/+}$ mice at 4 and 18 months of age. (A) Spontaneous mutant frequencies of the *red/gam* genes in the livers. (B) Spontaneous mutant frequencies in the *gpt* genes of the livers. Error bars represent standard error values. (C) Effect of *Parp-1* deficiency on the mutation spectrum of the *red/gam* genes in the liver at 18 months of age. Specific mutation frequencies in the *red/gam* genes of the liver are shown. Mean values and standard error values are presented for *Parp-1*$^{-/-}$ and *Parp-1*$^{+/+}$ mice ($n = 6$ and 4, respectively). (D) Distribution of single base deletion mutations in the *gam* gene of the livers at 18 months of age. Single base deletions were observed on non-repeat, or 2–3 base repeats, or 4–6 base repeats as indicated in the figure as repeat length $(N)_n$ of 1, 2, 4–6, respectively.

Parp-1$^{-/-}$ mice, but not in *Parp-1*$^{+/+}$ mice in the liver at 18 months old. As shown in Table 1, the frequencies of complex-type deletions in *Parp-1*$^{-/-}$ mice showed a higher tendency than those in *Parp-1*$^{+/+}$ mice, although it is not statistically significant ($p = 0.224$). The structures of complex-type mutations of *Parp-1*$^{-/-}$ mice observed at 18 months of age are shown in Table 2. Two complex-type deletions observed in *Parp-1*$^{-/-}$ mice accompanied both small insertions and microhomologous sequences at deletion junctions (Table 2). It is of note that complementary nucleotides AAA (G61-1-3) or TT (G93-2-3) (marked with upper lines in Table 2) are present at the 5′ position to these microhomologous deletion junctions in each case.

Table 1
Spectrum of the mutations of two bases or more in the *red/gam* genes in the liver and brain of *Parp-1*$^{-/-}$ mice at 18 months old.

Tissue	Deletion	*Parp-1*$^{+/+}$		*Parp-1*$^{-/-}$	
		Mutation frequency ($\times 10^{-6}$)	No. of mutants (MEJ/Non-MEJ)	Mutation frequency ($\times 10^{-6}$)	No. of mutants (MEJ/Non-MEJ)
Liver	Simple	0.34 ± 0.21	3 (2/1)	0.96 ± 0.27	13 (6/7)
	Complex	<0.16	0	0.13 ± 0.08	2 (2/0)
	with small insertion[a]	<0.16	0	0.13 ± 0.08	2 (2/0)
	with recombination	<0.16	0	<0.13	0
Brain	Simple	0.15 ± 0.15	1 (0/1)	0.32 ± 0.14	3 (2/1)
	Complex	<0.18	0	0.32 ± 0.14	3 (1/1)*
	with small insertion	<0.18	0	0.19 ± 0.12	2 (1/1)
	with recombination	<0.18	0	0.12 ± 0.12	1

MEJ; microhomology-mediated end joining. Non-MEJ; non-microhomology-mediated end joining.
[a] Small insertion represents 4–9 bp insertion.
* One of the mutants could not be classified into MEJ or non-MEJ type.

3.3. Mutation frequencies of the red/gam gene in the brains at 4 and 18 months of age

Parp-1$^{-/-}$ mice showed 1.5-fold higher mutant frequencies compared to *Parp-1*$^{+/+}$ mice ($p = 0.047$) in the brains at 4 months of age (Fig. 2A). The brains of *Parp-1*$^{-/-}$ mice showed a 2.2-fold higher tendency of mutant frequencies than those in *Parp-1*$^{+/+}$ mice ($p = 0.088$) at 18 months of age (Fig. 2A). The tendency of age-dependent slight increase in the mutant frequency in the brain was observed in *Parp-1*$^{-/-}$ but not in *Parp-1*$^{+/+}$ mice, as mentioned earlier in the case with the liver. Analysis of the mutation spectrum in the brain (Fig. 2C) revealed some differences from that of the livers. In the brain, a tendency of increase in base substitution and deletion mutations of two bases or more was observed in *Parp-1*$^{-/-}$ mice compared to *Parp-1*$^{+/+}$ mice (base substitution: $p = 0.055$, deletion mutation: $p = 0.11$). Different from the cases in the liver, the frequency of single base deletions at non-repeat or 2–3 bp repeats is not increased in the brain of *Parp-1*$^{-/-}$ mice at 18 months of age compared to *Parp-1*$^{+/+}$ mice (Fig. 2C).

3.4. Lower mutation frequencies of the gpt gene in the brains of Parp-1$^{-/-}$ than Parp-1$^{+/+}$ mice at 4 months of age and age-dependent increase

Of note, mutant frequencies of the *gpt* gene in the brains of *Parp-1*$^{-/-}$ mice were lower than those of *Parp-1*$^{+/+}$ mice ($p = 0.009$) at 4 months of age (Fig. 2B). No pathological changes in the brains were observed in *Parp-1*$^{-/-}$ and *Parp-1*$^{+/+}$ mice. Mutation spectra in the brains of *Parp-1*$^{-/-}$ mice showed a lower frequency of G:C to A:T base transition mutations ($p = 0.047$) as well as deletion mutations ($p = 0.034$) compared to *Parp-1*$^{+/+}$ mice at 4 months old (Fig. 2D).

The *gpt* mutant frequency showed an increase at 18 months of age in the *Parp-1*$^{-/-}$ but not in *Parp-1*$^{+/+}$ mice ($p = 0.011$, Fig. 2B). There was no difference in the mutant frequencies of the *gpt* gene in the brain between *Parp-1*$^{-/-}$ and *Parp-1*$^{+/+}$ mice at 18 months of age (Fig. 2B).

Comparison of the mutation spectra between 4 and 18 months of age in *Parp-1*$^{-/-}$ mice suggests a tendency of age-dependent increase in the frequencies of deletion mutations ($p = 0.068$, Fig. 2D). A tendency of increase of point mutation ($p = 0.144$) is also noticed, suggesting that Parp-1 may be involved in suppressing age-dependent introduction of point mutations in the brain.

4. Discussion

Spontaneous *gpt* and *red/gam* mutant frequencies are reported to be around $2–6 \times 10^{-6}$ and $1–5 \times 10^{-6}$, respectively, in *gpt* delta mice of C57BL/6 genetic background [23,24]. In this study, the spontaneous mutation frequencies of *gpt* and *red/gam* mutant frequencies in the liver and the brain of *Parp-1*$^{+/+}$ are both around 2×10^{-6} at 4 months of age and thus consistent with the previous reports. The mutant frequency of the *gpt* gene in the small intestine

Table 2
Junctional sequences of complex-type mutations in the liver and brain of *Parp-1*$^{-/-}$ mice at 18 months old.

Tissue	Mutant ID[a]	Original sequence in lambdaEG10		Junctional sequence of mutation	Deletion/insertion size (nucleotide position in lambdaEG10)
Liver	G61-1-3	5′-GTCATCAAACgcac	ttttGCTGGCCCCG-3′	5′-GTCATCAAACacacGCTGGCCCCG-3′	20 bp deletion + 4 bp insertion (25021 - 25040)
		3′-CAGTAGTTTGcgtg	aaaaCGACCGGGGC-5′	3′-CAGTAGTTTGtgtgCGACCGGGGC-5′	
	G93-2-3	5′-CCGTGGCGTTgcaa	ataaGCGTTCATGG-3′	5′-CCGTGGCGTTttgctgGCGTTCATGG-3′	149 bp deletion + 6 bp insertion (25058 - 25206)
		3′-GGCACCGCAAcgtt	tattCGCAAGTACC-5′	3′-GGCACCGCAAaacgacCGCAAGTACC-5′	
Brain	G61-1-1	5′-TTCATTAGACttat	tagtGAATGCTTTT-3′	5′-TTCATTAGACaaattaGAATGCTTTT-3′	3694 bp deletion + 6 bp insertion (21600 - 25293)
		3′-AAGTAATCTGaata	atcaCTTACGAAAA-5′	3′-AAGTAATCTGtttaatCTTACGAAAA-5′	
	G94-1-1	5′-TGTCTGCATGgaga	aatcGATTTTCCCT-3′	5′-TGTCTGCATGagaccagaaGATTTTCCCT-3′	3805 bp deletion + 9 bp insertion (21682 - 25486)
		3′-ACAGACGTACctct	ttagCTAAAAGGGA-5′	3′-CGTACCTCTGtctggtcttCTAAAAGGGA-5′	
	G93-2-4		acgcGCCCAGCTCT-3′	5′-taagagtcagGCCCAGCTCT-3′	Recombination with unknown sequence
			tgcgCGGGTCGAGA-5′	3′-attctcagtcCGGGTCGAGA-5′	

[a]ID; Identification number. Red and blue letters indicate deleted and inserted sequences, respectively. Letters in the box are microhomologous sequences. Upperlines show complementary mononucleotide sequences at 5′ positions of the microhomologous sequences.

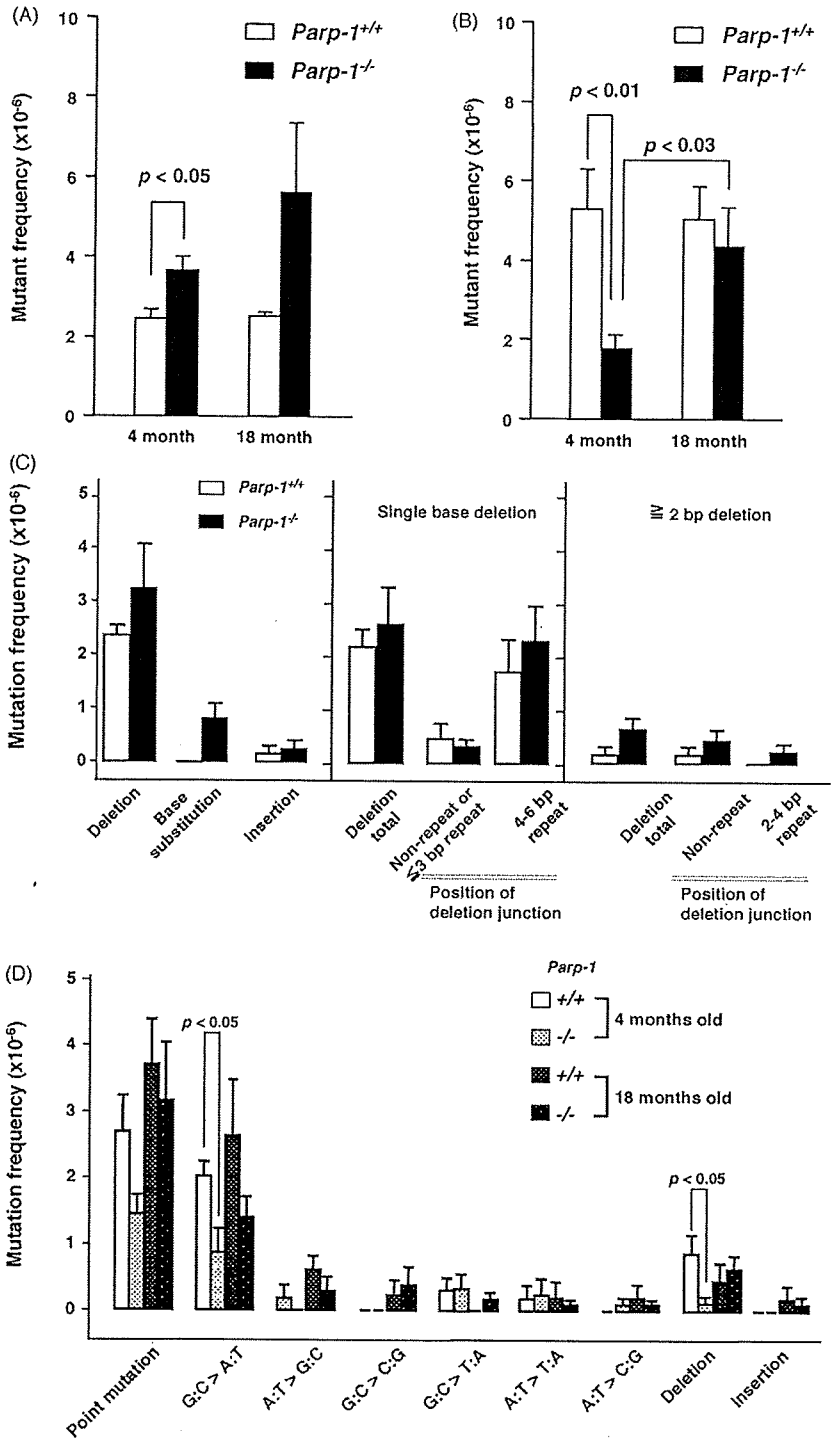

Fig. 2. Spontaneous mutant frequencies of the *red/gam* and *gpt* genes in the brain of *Parp-1*$^{-/-}$ and *Parp-1*$^{+/+}$ mice at 4 and 18 months of age. (A) Spontaneous mutant frequencies of the *red/gam* genes. (B) Spontaneous mutant frequencies in the *gpt* genes. Error bars represent standard error values. (C) Mutation spectra of the *red/gam* genes in the brain of *Parp-1*$^{-/-}$ and *Parp-1*$^{+/+}$ mice at 18 months of age. (D) Mutation spectra of the *gpt* genes in the brain of *Parp-1*$^{-/-}$ and *Parp-1*$^{+/+}$ mice at 4 and 18 months of age.

of *gpt* delta transgenic mice of mixed genetic background of SWR and C57BL/6 is reported to be 2.5×10^{-5} [22], which is higher compared to other reports on *gpt* delta mice [23,24]. This difference could be due to the mouse strain, tissues or other factors. From 4 to 18 months of age, the mutant frequency of the *gpt* gene in *Parp-1*$^{+/+}$ mice increased 2-fold. The mutant frequency of the *lacZ* marker gene in the liver is around 5×10^{-6} at 4–6 months of age and 1.2×10^{-5} at 24–34 months of age in wild-type mice [19]. Therefore age-dependent 2-fold increase in mutant frequency is consistently observed both in the *gpt* and *lacZ* [19] genes. On the other hand, size change mutations in the liver detected by the *lacZ* gene system did not significantly increase before 25–27 months [19] but

increased thereafter. Increase of mutant frequency in the *red/gam* gene in *Parp-1*$^{+/+}$ mice at 18 months of age, which detects deletion mutation, was not observed in the liver, being consistent with the results in the *lacZ* gene [19]. In the *lacZ* gene system, the target size is around 3000 bp, whereas that in the *gpt* and *red/gam* gene (Spi$^-$ assay) are around 456 and 417 bp, respectively. The smaller size of the target sequences of the *gpt* and *red/gam* genes could be also responsible for the lower spontaneous mutant frequencies.

In this study, *Parp-1*$^{-/-}$ mice showed a tendency of higher frequencies of spontaneous deletion mutations in the *red/gam* gene, including complex-type deletions in the liver ($p = 0.20$) and brain ($p = 0.29$) at 18 months of age.

The single base deletion mutations at non-repeat or short repeat sequences of the *red/gam* gene showed a 5.8-fold increase ($p = 0.031$) in the liver of *Parp-1*$^{-/-}$ mice compared to *Parp-1*$^{+/+}$ mice at 18 months of age. The frequency of deletion mutations of two bases or more also showed a 3.2-fold higher tendency in the *Parp-1*$^{-/-}$ than in the *Parp-1*$^{+/+}$ liver ($p = 0.084$). We observed complex-type deletions in the livers and brains of *Parp-1*$^{-/-}$ but not in *Parp-1*$^{+/+}$ mice at 18 months old.

8-Oxodeoxyguanosine (8-oxodG) is one outcome of major oxidative DNA damage [31]. The 8-oxodG levels in DNA of the liver, lungs, and small intestine in double knockout mice lacking both 8-oxoguanine DNA glycosylase 1 (*Ogg1*) and Mut Y homologue (*Myh*) genes increased linearly between 4 and 14 months of age [32]. 8-OxodG and SSB, which are expected outcomes of major endogenous DNA damage, are preferentially repaired by BER. Parp-1 is shown to be involved in BER and deletion mutations of single base and larger sizes of deletion as well as complexed-type were increased in *Parp-1*$^{-/-}$ mice after treatment with an alkylating agent, BHP [20]. The frequency of single base deletion mutations at non-repeat or short repeat sequences of the *red/gam* gene also increased 2.9-fold in *Parp-1*$^{-/-}$ mice compared to *Parp-1*$^{+/+}$ mice ($p = 0.043$) in the liver after treatment of the alkylating agent, whereas no difference in the frequency of single base deletion at 4–6 bp of mononucleotide repeats was observed between genotypes [20]. Therefore the spectra of single base deletions in the liver of *Parp-1*$^{-/-}$ mice at advanced age and after treatment with the alkylating agent are similar to each other. Stalled BER in the absence of Parp-1 at a SSB introduced step may further cause deletion mutations after treatment with an alkylating agent [20]. Therefore, there is a possibility that deletion mutation is also caused through BER induced by endogenous DNA damage during aging in *Parp-1*$^{-/-}$ mice. After introduction of SSB during BER, lack of Parp-1 may induce stall or delay in BER and terminal nucleotides may be destabilized and lost under *Parp-1* deficiency by exonuclease activity (Fig. 3). Collision between SSB and replication forks induces double strand breaks (DSBs) [33]. Two SSBs on opposite strands within at least 30 nt could resolve into a DSB [34]. Therefore, an increase of spontaneous DSBs might also be caused by the presence of SSBs during replication fork progression or defective BER under *Parp-1* deficiency.

Deletion mutations including single base deletions may be also produced during imprecise non-homologous end joining (NHEJ). In NHEJ reconstituted systems that utilize DSB substrates, it is shown that deletion or insertion of single bases as well as larger sizes occurs during the NHEJ process [35–37]. In chicken DT-40 cells, Parp-1 negatively regulates the NHEJ process by inhibiting Ku70/Ku80 action, and *Parp-1* deficiency causes an increase of NHEJ frequency [38]. However, DT-40 cells are known to have high HR levels compared to typical mammalian somatic cells. Using mouse embryonic fibroblast or CHO cells, it is demonstrated that Parp-1 competes with Ku for DSB binding and is shown to be involved in a backup pathway of classical NHEJ pathway with DNA ligase III [39]. Therefore, as shown in Fig. 3, during a NHEJ process of DSB, terminal nucleotides may be destabilized in the absence of Parp-1, and resection of bases by the exonuclease may lead to deletion mutation.

It is also notable that the frequency of single base deletions at 4–6 bp mononucleotide repeats did not show a difference between either genotypes in the livers and brains. Single base deletion mutations at 4–6 bp of mononucleotide repeats, namely at run sequences, might be caused by slippage error during DNA replication or repair reaction. The results suggest that Parp-1 is not essential to suppress these slippage type errors induced during aging.

Two complex-type deletions observed in *Parp-1*$^{-/-}$ mice accompanied small insertions as well as microhomologous sequences at deletion junctions, suggesting that these mutations could be

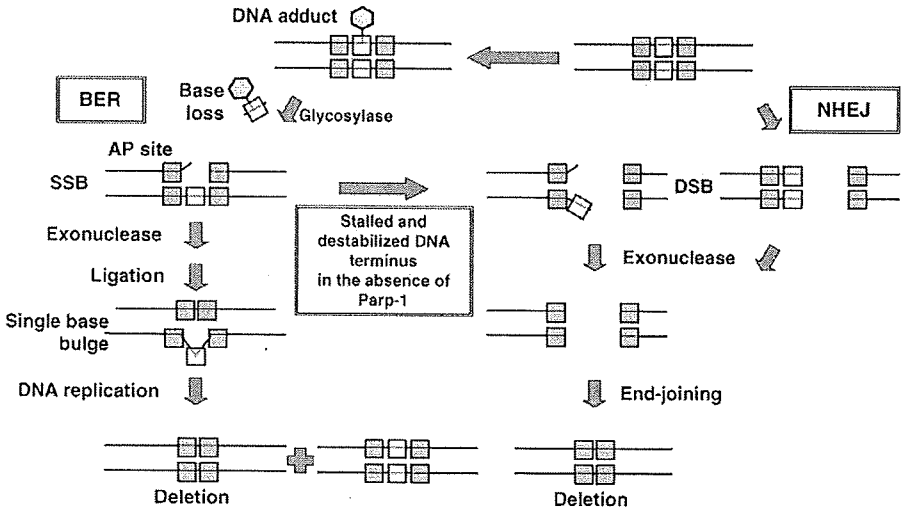

Fig. 3. A model for augmented development of deletion mutation through imprecise BER or NHEJ process in the absence of Parp-1. During BER, after single strand breaks are introduced following damaged base removal, the DNA terminus may be destabilized in the absence of Parp-1. Base loss could occur by the DNA exonuclease activity. When misannealing and ligation occur, the deletion will be fixed by subsequent DNA replication. Stalled BER reaction in the absence of Parp-1 on single strand breaks may also cause DSB and may induce switching to a NHEJ reaction and subsequently base loss will be fixed by end-joining process. During DSB repair process by NHEJ, base loss frequency might be augmented at the destabilized DNA terminus in the absence of Parp-1.

caused by insertion of a few nucleotides during microhomologous end-joining (MEJ)-type reactions. A few complementary bases are present at the 5′ position of the microhomologous sequences (marked with upper lines in Table 2). During the end-joining process, after resection of strand ends, transient base-pairing at microhomologous sequences may occur and a few complementary bases at the 5′ position may also form base-pairing. In the absence of Parp-1, these base-pairings may be destabilized and resection and insertion of a few bases may tend to occur in the livers. Consistently of all seven simple-type deletions of two bases or more observed in the livers of *Parp-1*$^{-/-}$ mice (Table 1), none harbored a few complementary bases at the 5′ position of the microhomologous sequences (data not shown). On the other hand, in two simple-type deletions of two bases or more in *Parp-1*$^{+/+}$ mice, one deletion harbored a few complementary bases at the 5′ position of the microhomologous deletion junctions (Table 1).

In the brain, one out of three complex-type deletions of *Parp-1*$^{-/-}$ mice harbored microhomologous deletion junctions but did not harbor complementary bases at 5′ positions of the microhomologous deletion junctions. This point should be further evaluated by analyzing deletion mutations induced after treatment with various types of DNA damaging agents in different tissues.

The xeroderma pigmentosum complementation group A (Xpa) plays an important role in nucleotide excision repair (NER) and *Xpa*-deficient mice also show higher spontaneous mutant frequencies in the liver at advanced ages [40]. In fact, *Xpa*-deficient mice show an increased frequency of hepatocellular adenomas at older ages [34]. It is thus possible that endogenous DNA damage repairable by NER may occur during aging. However, no increase in the susceptibility to carcinogenesis induced in *Parp-1*$^{-/-}$ mice by 4-nitrosoquinoline1-oxide [41], which induces bulky DNA adducts, suggests that Parp-1 is not involved in NER.

Most liver cells stay in the G0 phase and they usually enter the cell division cycle after various stimulating events. An augmented frequency of DNA replication, like that in preneoplastic lesions, can also increase the chance of DSBs and may increase the frequency of deletions. Two of six *Parp-1*$^{-/-}$ mice used in the mutation analysis harbored tumors in the liver and the tumor regions were not included for DNA isolation. Because the frequencies and spectrum of mutations in the *gpt* or *red/gam* genes were unbiased in each mouse, we can exclude the possibility that the tissues used for isolation of DNA contained monoclonally proliferating preneoplastic lesions or other cycling cells.

It is also possible that an increased frequency of cell division may be causative of augmented frequency of DSBs and may result in a higher frequency of deletion mutation. However, if this is true, the observed mutation spectrum is expected to be the same between the genotypes. We could rule out this possibility because we observed different spectra of deletion mutations between the genotypes.

Unexpectedly we also found a 3-fold lower frequency of point mutations in adolescent *Parp-1*$^{-/-}$ compared to *Parp-1*$^{+/+}$ mice in the brain ($p = 0.009$). An age-dependent increase in the mutant frequency in *Parp-1*$^{-/-}$ mice was also shown ($p = 0.011$). Lower frequencies of G:C to A:T type mutation and deletion mutation in *Parp-1*$^{-/-}$ mice suggest that Parp-1 may be positively involved imprecise repair pathways which cause base substitution mutation of G:C to A:T and deletion mutation in the brain.

In conclusion, this result supports the view that Parp-1 is involved in suppressing imprecise repair of endogenous DNA damage leading to deletion mutation during aging in the liver and brain. *Parp-1*$^{-/-}$ mice show increased incidence of hepatocellular tumors at 18–24 months of ages [13]. The present results suggest a substantial role of Parp-1 in the maintenance of genomic stability and suppression of carcinogenesis during aging.

Conflict of interest

The authors declare that there are no conflicts of interest.

Acknowledgements

We are grateful to M. Abe for technical assistance, M. Yanagihara for maintenance of the animals and H. Suzuki and S. Gotoh for helpful suggestions on the manuscript. This work was supported in part by a Grant-in-Aid for the Cancer Research from the Ministry of Health, Labour and Welfare, a Grand-in-Aid from Third Term Comprehensive 10-Year Strategy for Cancer Control, and a Grant-in-Aid for Scientific Research from the Ministry of Education, Science, Sports, and Culture of Japan (16-11804).

References

[1] M. Masson, C. Niedergang, V. Schreiber, S. Muller, J. Menissier-de Murcia, G. de Murcia, XRCC1 is specifically associated with poly(ADP-ribose) polymerase and negatively regulates its activity following DNA damage, Mol. Cell. Biol. 18 (1998) 3563–3571.
[2] C. von Kobbe, J.A. Harrigan, V. Schreiber, P. Stiegler, J. Piotrowski, L. Dawut, V.A. Bohr, Poly(ADP-ribose) polymerase 1 regulates both the exonuclease and helicase activities of the Werner syndrome protein, Nucleic Acids Res. 32 (2004) 4003–4014.
[3] C. von Kobbe, J.A. Harrigan, A. May, P.L. Opresko, L. Dawut, W.H. Cheng, V.A. Bohr, Central role for the Werner syndrome protein/poly(ADP-ribose) polymerase 1 complex in the poly(ADP-ribosyl)ation pathway after DNA damage, Mol. Cell. Biol. 23 (2003) 8601–8613.
[4] S. Galande, T. Kohwi-Shigematsu, Poly(ADP-ribose) polymerase and Ku autoantigen form a complex and synergistically bind to matrix attachment sequences, J. Biol. Chem. 274 (1999) 20521–20528.
[5] B. Li, S. Navarro, N. Kasahara, L. Comai, Identification and biochemical characterization of a Werner's syndrome protein complex with Ku70/80 and poly(ADP-ribose) polymerase-1, J. Biol. Chem. 279 (2004) 13659–13667.
[6] L. Lan, S. Nakajima, Y. Oohata, M. Takao, S. Okano, M. Masutani, S.H. Wilson, A. Yasui, In situ analysis of repair processes for oxidative DNA damage in mammalian cells, Proc. Natl. Acad. Sci. U.S.A. 101 (2004) 13738–13743.
[7] S. Okano, L. Lan, K.W. Caldecott, T. Mori, A. Yasui, Spatial and temporal cellular responses to single-strand breaks in human cells, Mol. Cell. Biol. 23 (2003) 3974–3981.
[8] F. Le Page, V. Schreiber, C. Dherin, G. De Murcia, S. Boiteux, Poly(ADP-ribose) polymerase-1 (PARP-1) is required in murine cell lines for base excision repair of oxidative DNA damage in the absence of DNA polymerase beta, J. Biol. Chem. 278 (2003) 18471–18477.
[9] J.B. Leppard, Z. Dong, Z.B. Mackey, A.E. Tomkinson, Physical and functional interaction between DNA ligase IIIalpha and poly(ADP-Ribose) polymerase 1 in DNA single-strand break repair, Mol. Cell. Biol. 23 (2003) 5919–5927.
[10] M. Tsutsumi, M. Masutani, T. Nozaki, O. Kusuoka, T. Tsujiuchi, H. Nakagama, H. Suzuki, Y. Konishi, T. Sugimura, Increased susceptibility of poly(ADP-ribose) polymerase-1 knockout mice to nitrosamine carcinogenicity, Carcinogenesis 22 (2001) 1–3.
[11] T. Nozaki, H. Fujihara, M. Watanabe, M. Tsutsumi, K. Nakamoto, O. Kusuoka, N. Kamada, H. Suzuki, H. Nakagama, T. Sugimura, M. Masutani, *Parp-1* deficiency implicated in colon and liver tumorigenesis induced by azoxymethane, Cancer Sci. 94 (2003) 497–500.
[12] A. Gunji, A. Uemura, M. Tsutsumi, T. Nozaki, O. Kusuoka, K. Omura, H. Suzuki, H. Nakagama, T. Sugimura, M. Masutani, *Parp-1* deficiency does not increase the frequency of tumors in the oral cavity and esophagus of ICR/129Sv mice by 4-nitroquinoline 1-oxide, a carcinogen producing bulky adducts, Cancer Lett. 241 (2005) 87–92.
[13] W.M. Tong, U. Cortes, M.P. Hande, H. Ohgaki, L.R. Cavalli, P.M. Lansdorp, B.R. Haddad, Z.Q. Wang, Synergistic role of Ku80 and poly(ADP-ribose) polymerase in suppressing chromosomal aberrations and liver cancer formation, Cancer Res. 62 (2002) 6990–6996.
[14] W.M. Tong, U. Cortes, Z.Q. Wang, Poly(ADP-ribose) polymerase: a guardian angel protecting the genome and suppressing tumorigenesis, Biochim. Biophys. Acta 1552 (2001) 27–37.
[15] W.M. Tong, H. Ohgaki, H. Huang, C. Granier, P. Kleihues, Z.Q. Wang, Null mutation of DNA strand break-binding molecule poly(ADP-ribose) polymerase causes medulloblastomas in p53(−/−) mice, Am. J. Pathol. 162 (2003) 343–352.
[16] M.E. Dolle, W.K. Snyder, J.A. Gossen, P.H. Lohman, J. Vijg, Distinct spectra of somatic mutations accumulated with age in mouse heart and small intestine, Proc. Natl. Acad. Sci. U.S.A. 97 (2000) 8403–8408.
[17] K.A. Hill, V.L. Buettner, A. Halangoda, M. Kunishige, S.R. Moore, J. Longmate, W.A. Scaringe, S.S. Sommer, Spontaneous mutation in Big Blue mice from fetus to old age: tissue-specific time courses of mutation frequency but similar mutation types, Environ. Mol. Mutagen. 43 (2004) 110–120.
[18] T. Ono, H. Ikehata, S. Nakamura, Y. Saito, Y. Hosoi, Y. Takai, S. Yamada, J. Onodera, K. Yamamoto, Age-associated increase of spontaneous mutant frequency and

molecular nature of mutation in newborn and old lacZ-transgenic mouse, Mutat. Res. 447 (2000) 165–177.
[19] M.E. Dolle, H. Giese, C.L. Hopkins, H.J. Martus, J.M. Hausdorff, J. Vijg, Rapid accumulation of genome rearrangements in liver but not in brain of old mice, Nat. Genet. 17 (1997) 431–434.
[20] A. Shibata, N. Kamada, K. Masumura, T. Nohmi, S. Kobayashi, H. Teraoka, H. Nakagama, T. Sugimura, H. Suzuki, M. Masutani, *Parp-1* deficiency causes an increase of deletion mutations and insertions/rearrangements in vivo after treatment with an alkylating agent, Oncogene 24 (2005) 1328–1337.
[21] T. Nohmi, M. Katoh, H. Suzuki, M. Matsui, M. Yamada, M. Watanabe, M. Suzuki, N. Horiya, O. Ueda, T. Shibuya, H. Ikeda, T. Sofuni, A new transgenic mouse mutagenesis test system using Spi- and 6-thioguanine selections, Environ. Mol. Mutagen. 28 (1996) 465–470.
[22] R.R. Swiger, L. Cosentino, K.I. Masumura, T. Nohmi, J.A. Heddle, Further characterization and validation of gpt delta transgenic mice for quantifying somatic mutations in vivo, Environ. Mol. Mutagen. 37 (2001) 297–303.
[23] K. Masumura, K. Kuniya, T. Kurobe, M. Fukuoka, F. Yatagai, T. Nohmi, Heavy-ion-induced mutations in the *gpt* delta transgenic mouse: comparison of mutation spectra induced by heavy-ion, X-ray, and gamma-ray radiation, Environ. Mol. Mutagen. 40 (2002) 207–215.
[24] K. Masumura, T. Nohmi, Spontaneous mutagenesis in rodents: spontaneous gene mutations identified by neutral reporter genes in *gpt* delta transgenic mice and rats, J. Health Sci. 55 (2009) 40–49.
[25] K. Masumura, K. Matsui, M. Yamada, M. Horiguchi, K. Ishida, M. Watanabe, O. Ueda, H. Suzuki, Y. Kanke, K.R. Tindall, K. Wakabayashi, T. Sofuni, T. Nohmi, Mutagenicity of 2-amino-1-methyl-6-phenylimidazo [4,5-b]pyridine (PhIP) in the new *gpt* delta transgenic mouse, Cancer Lett. 143 (1999) 241–244.
[26] F. Yatagai, T. Kurobe, T. Nohmi, K. Masumura, T. Tsukada, H. Yamaguchi, K. Kasai-Eguchi, N. Fukunishi, Heavy-ion-induced mutations in the gpt delta transgenic mouse: effect of p53 gene knockout, Environ. Mol. Mutagen. 40 (2002) 216–225.
[27] A. Shibata, M. Masutani, T. Nozaki, N. Kamada, H. Fujihara, K. Masumura, H. Nakagama, T. Sugimura, S. Kobayashi, H. Suzuki, T. Nohmi, Improvement of the Spi-assay for mutations in *gpt* delta mice by including magnesium ions during plaque formation, Environ. Mol. Mutagen. 41 (2003) 370–372.
[28] T. Nohmi, M. Suzuki, K. Masumura, M. Yamada, K. Matsui, O. Ueda, H. Suzuki, M. Katoh, H. Ikeda, T. Sofuni, Spi(-) selection: an efficient method to detect gamma-ray-induced deletions in transgenic mice, Environ. Mol. Mutagen. 34 (1999) 9–15.
[29] A. Shibata, M. Masutani, N. Kamada, K. Masumura, H. Nakagama, S. Kobayashi, H. Teraoka, H. Suzuki, T. Nohmi, Efficient method for mapping and characterizing structures of deletion mutations in *gpt* delta mice using Southern blot analysis with oligo DNA probes, Environ. Mol. Mutagen. 43 (2004) 204–207.
[30] K. Masumura, M. Matsui, M. Katoh, N. Horiya, O. Ueda, H. Tanabe, M. Yamada, H. Suzuki, T. Sofuni, T. Nohmi, Spectra of *gpt* mutations in ethylnitrosourea-treated and untreated transgenic mice, Environ. Mol. Mutagen. 34 (1999) 1–8.
[31] H. Kasai, P.F. Crain, Y. Kuchino, S. Nishimura, A. Ootsuyama, H. Tanooka, Formation of 8-hydroxyguanine moiety in cellular DNA by agents producing oxygen radicals and evidence for its repair, Carcinogenesis 7 (1986) 1849–1851.
[32] M.T. Russo, G. De Luca, P. Degan, E. Parlanti, E. Dogliotti, D.E. Barnes, T. Lindahl, H. Yang, J.H. Miller, M. Bignami, Accumulation of the oxidative base lesion 8-hydroxyguanine in DNA of tumor-prone mice defective in both the *Myh* and *Ogg1* DNA glycosylases, Cancer Res. 64 (2004) 4411–4414.
[33] T. Furuta, H. Takemura, Z.Y. Liao, G.J. Aune, C. Redon, O.A. Sedelnikova, D.R. Pilch, E.P. Rogakou, A. Celeste, H.T. Chen, A. Nussenzweig, M.I. Aladjem, W.M. Bonner, Y. Pommier, Phosphorylation of histone H2AX and activation of Mre11, Rad50, and Nbs1 in response to replication-dependent DNA double-strand breaks induced by mammalian DNA topoisomerase I cleavage complexes, J. Biol. Chem. 278 (2003) 20303–20312.
[34] S. Vispe, M.S. Satoh, DNA repair patch-mediated double strand DNA break formation in human cells, J. Biol. Chem. 275 (2000) 27386–27392.
[35] F. Liang, M. Han, P.J. Romanienko, M. Jasin, Homology-directed repair is a major double-strand break repair pathway in mammalian cells, Proc. Natl. Acad. Sci. U.S.A. 95 (1998) 5172–5177.
[36] M. Honma, M. Sakuraba, T. Koizumi, Y. Takashima, H. Sakamoto, M. Hayashi, Non-homologous end-joining for repairing I-SceI-induced DNA double strand breaks in human cells, DNA Repair (Amst.) 6 (2007) 781–788.
[37] Y. Ma, H. Lu, B. Tippin, M.F. Goodman, N. Shimazaki, O. Koiwai, C.L. Hsieh, K. Schwarz, M.R. Lieber, A biochemically defined system for mammalian nonhomologous DNA end joining, Mol. Cell 16 (2004) 701–713.
[38] H. Hochegger, D. Dejsuphong, T. Fukushima, C. Morrison, E. Sonoda, V. Schreiber, G.Y. Zhao, A. Saberi, M. Masutani, N. Adachi, H. Koyama, G. de Murcia, S. Takeda, Parp-1 protects homologous recombination from interference by Ku and Ligase IV in vertebrate cells, EMBO J. 25 (2006) 1305–1314.
[39] M. Wang, W. Wu, W. Wu, B. Rosidi, L. Zhang, H. Wang, G. Iliakis, PARP-1 and Ku compete for repair of DNA double strand breaks by distinct NHEJ pathways, Nucleic Acids Res. 34 (2006) 6170–6182.
[40] H. Giese, M.E. Dolle, A. Hezel, H. van Steeg, J. Vijg, Accelerated accumulation of somatic mutations in mice deficient in the nucleotide excision repair gene *XPA*, Oncogene 18 (1999) 1257–1260.
[41] A. de Vries, C.T. van Oostrom, P.M. Dortant, R.B. Beems, C.F. van Kreijl, P.J. Capel, H. van Steeg, Spontaneous liver tumors and benzo[a]pyrene-induced lymphomas in *XPA*-deficient mice, Mol. Carcinogen. 19 (1997) 46–53.

Fungal Genetics and Biology xxx (2010) xxx–xxx

Contents lists available at ScienceDirect

Fungal Genetics and Biology

journal homepage: www.elsevier.com/locate/yfgbi

PARP is involved in replicative aging in *Neurospora crassa*

Gregory O. Kothe [a,*,2], Maki Kitamura [b,1,2], Mitsuko Masutani [c], Eric U. Selker [a], Hirokazu Inoue [b]

[a] *Institute of Molecular Biology, University of Oregon, Eugene, OR 97403, United States*
[b] *Lab of Genetics, Department of Regulation Biology, Saitama University, Saitama City 338-8570, Japan*
[c] *Biochemistry Division, National Cancer Center Research Institute, Tokyo 104-0045, Japan*

ARTICLE INFO

Article history:
Received 8 July 2009
Accepted 29 December 2009
Available online xxxx

Keywords:
PARP
Aging
Neurospora
Chromatin
DNA repair

ABSTRACT

Modification of proteins by the addition of poly(ADP-ribose) is carried out by poly(ADP-ribose) polymerases (PARPs). PARPs have been implicated in a wide range of biological processes in eukaryotes, but no universal function has been established. A study of the *Aspergillus nidulans* PARP ortholog (PrpA) revealed that the protein is essential and involved in DNA repair, reminiscent of findings using mammalian systems. We found that a Neurospora PARP orthologue (NPO) is dispensable for cell survival, DNA repair and epigenetic silencing but that replicative aging of mycelia is accelerated in an *npo* mutant strain. We propose that PARPs may control aging as proposed for Sirtuins, which also consume NAD+ and function either as mono(ADP-ribose) transferases or protein deacetylases. PARPs may regulate aging by impacting NAD+/NAM availability, thereby influencing Sirtuin activity, or they may function in alternative NAD+-dependent or NAD+-independent aging pathways.

1. Introduction

Poly(ADP-ribose) polymerases (PARPs) are ADP-ribose transferases that catalyze the formation of both linear and branched polymers of ADP-ribose (PAR) on target proteins. PAR is covalently linked to the γ-carboxy group of glutamic acid residues at acceptor sites (Burzio et al., 1979; Riquelme et al., 1979). Poly(ADP-ribosylation) (PARylation) consumes nicotinamide adenine dinucleotide (NAD+) and generates nicotinamide (NAM). The addition of PAR to proteins is thought to have dramatic effects on their catalytic activities, as well as on potential protein–protein and protein–nucleic acid interactions (Burkle, 2000; D'Amours et al., 1999; Kraus and Lis, 2003). Recently a number of different proteins have been identified that bind to PAR both *in vitro* and *in vivo*, including proteins containing Macro domains and proteins containing novel poly(ADP-ribose)-binding zinc finger (PBZ) motifs (Ahel et al., 2008; Karras et al., 2005). In higher eukaryotes PARylation is reversible through the action of PAR glycohydrolases (PARG), which are active in a variety of subcellular compartments, and are thought to be important in regulation of cell death after DNA damage (Ame et al., 2009a,b). Thus, the principle players in PARylation thus far identified are the PARPs, PARG and PAR binding proteins.

PARP homologs have been identified in plants, metazoans, protists and filamentous fungi, but not in the yeasts, while PARG homologs have been identified in all eukaryotes, excluding fungi. PARPs and PARylation impact a variety of biological processes including development, transcriptional regulation, chromatin structure, epigenetic phenomena, DNA repair, mitosis, genome stability, neuronal function, cell death and aging (Beneke and Burkle, 2004, 2007; Bouchard et al., 2003; Boulu et al., 2001; Burkle, 2000, 2001a; Burkle et al., 2005; Chiarugi and Moskowitz, 2002; D'Amours et al., 1999; Herceg and Wang, 2001; Hong et al., 2004; Jeggo, 1998; Kim et al., 2005; Kraus and Lis, 2003; Pieper et al., 1999; Smulson et al., 2000).

The canonical PARP enzyme from mammals, PARP-1, has been implicated in both double and single strand break repair (DSB and SSB), as well as base excision repair (BER) (Burkle, 2001b; Dantzer et al., 1999; Masutani et al., 2003). In human and mouse cells, the majority of PARylation involves auto-modification of PARP-1 in response to DNA damage and PARP-1 has been described as a DNA damage sensor (D'Amours et al., 1999; de Murcia et al., 1997; Huletsky et al., 1989; Ogata et al., 1981). Residual PARylation is detectable in mouse embryonic fibroblast homozygous for PARP-1 null mutations (PARP-1$^{-/-}$) (Shieh et al., 1998) and this may reflect PARP-2, which has also been shown to PARylate in response to DNA damage (Ame et al., 1999). Both PARP-1$^{-/-}$ and PARP-2$^{-/-}$ mice are viable, but are sensitive to DNA damaging agents, and PARP-1$^{-/-}$ mice have inherent genomic instability (de Murcia et al., 1997; Menissier de Murcia et al., 2003; Trucco et al., 1998; Wang et al., 1995, 1997). PARP-1$^{-/-}$/PARP-2$^{-/-}$ mice die as embryos prior to E8.0, and PARP-1$^{+/-}$/PARP-2$^{-/-}$ female mice exhibit

* Corresponding author. Fax: +1 814 863 7024.
E-mail address: gok1@psu.edu (G.O. Kothe).
[1] Present address: HOKUTO Co. Nagano 381-0015, Japan.
[2] These authors contributed equally to this work.

1087-1845/$ - see front matter © 2010 Published by Elsevier Inc.
doi:10.1016/j.fgb.2009.12.012

X-chromosome instability, infertility, and higher levels of embryonic lethality (Menissier de Murcia et al., 2003). These results suggest that PARylation may be essential in higher eukaryotes.

A recent investigation using the filamentous fungus *Aspergillus nidulans* revealed the presence of a single PARP ortholog (PrpA) (Semighini et al., 2006). Disruption of the *prpA* gene was found to be lethal in haploid strains, and diploid strains carrying only a single copy of *prpA* had severe growth restrictions and were found to be sensitive to several mutagenic compounds (Semighini et al., 2006). These results suggest that the requirement of PARP for DNA repair and viability is conserved between animals and filamentous fungi.

In addition to evidence that PARPs and PARylation control diverse aspects of gene expression, DNA repair and genome stability, there are suggestions that PARP-1 is involved in controlling aging in metazoans. Grube and Burkle (1992) found a strong positive correlation between lifespan and the degree of PARP activity in leukocytes of 13 mammalian species. Long-lived species had higher levels of PARylation, but similar levels of PARP protein, implying greater enzyme activity (Grube and Burkle, 1992). In addition, the WRN protein, which is defective in individuals with the premature aging disorder Werner's syndrome, was found to physically and functionally interact with PARP-1 (Li et al., 2004; von Kobbe et al., 2004).

Research using microorganisms as models for aging has been dominated by studies in *Saccharomyces cerevisiae*. Replicative lifespan in *S. cerevisiae* is measured by determining the number of daughter cells an individual mother cell can produce (Mortimer and Johnston, 1959). Mutations in Silent Information Regulator (SIR) complex components were isolated in a genetic screen designed to identify genes that control this form of aging (Kennedy et al., 1995). In particular, the NAD+-dependent histone deacetylase Sir2 was shown to be a key regulator, acting to suppress recombination between rDNA repeats, thereby blocking the formation of extrachromosomal rDNA circles (ERCs), which are antagonistic to long replicative lifespan in budding yeast (Kaeberlein et al., 1999; Sinclair and Guarente, 1997).

Although Sir2-like proteins (Sirtuins) have been implicated in controlling lifespan in metazoans, regulation of ERC production is thought to be a yeast-specific aging mechanism (Rogina and Helfand, 2004; Tissenbaum and Guarente, 2001). Like Sir2 itself, Sirtuins are NAD+-dependent enzymes. Some Sirtuins act as mono(ADP-ribose) transferases (ARTS), others function as protein deacetylases, and some have both activities (Belenky et al., 2007). Genetic and biochemical investigations using *S. cerevisiae* have established that NAD+ and NAM levels impact replicative aging through regulation of Sir2 deacetylase activity (Gallo et al., 2004; Sandmeier et al., 2002). Additional studies have shown that lifespan extension by calorie restriction (CR) in *S. cerevisiae* involves Sir2, as well as the NAD+-dependent deacetylase Hst2, and is thus regulated by NAD+ and NAM levels as well (Anderson et al., 2003; Lamming et al., 2005; Lin et al., 2000, 2004). In addition, a yeast pathway for Sirtuin-independent lifespan extension by CR is also influenced by NAD+ and NAM availability (Tsuchiya et al., 2006). The fact that CR extends lifespan in higher eukaryotes, and that Sirtuins have been implicated in controlling aging in flies and worms suggests that NAD+ and NAM metabolism may be of general importance in the regulation of lifespan. While Sirtuins are present in all eukaryotes including the yeasts, additional ARTS, along with PARPs and cADP-ribose synthases exist in metazoans and filamentous fungi (Belenky et al., 2007). All of these enzymes are major consumers of NAD+, and might therefore be expected to impact aging. While aging studies in *S. cerevisiae* have provided many valuable insights, the involvement of certain key biological regulatory pathways that are common to many eukaryotic organisms, but absent from yeast, have not been adequately investigated. Research directed at understanding the roles of PARP and PARylation in aging of higher eukaryotes may be hindered by functional redundancy of multiple PARP enzymes and lethality of PARP mutants. Thus we chose to explore the function of PARP in the filamentous fungus *N. crassa*, which only has a single gene encoding this enzyme.

2. Materials and methods

2.1. Media and culturing conditions

N. crassa was cultured as described previously (Davis and DeSerres, 1970). Strains were grown in liquid Vogel's minimal media with 1.5% sucrose or 2% glucose and supplements were added where indicated. Solid media was the same but with 2% agar. Strains were grown on FGS (0.05% fructose, 0.05% glucose, 2% sorbose, 1X Vogel's salts, 2% agar) to induce colonial growth. The concentrations of supplements were as follows: 1× alanine (1 mg/ml), 1× anthranillic acid (140 μg/ml), 1× histidine (0.5 mg/ml), 1× lysine (0.6 mg/ml), 1× nicotinamide (10 μg/ml). Hygromycin was used in the range of 200 μg/ml to 1.5 mg/ml. Crosses were carried out on synthetic crossing medium with glucose or sucrose concentrations at 0.5% or 2.0%.

2.2. Southern and Northern blots

DNA was isolated from *N. crassa* and Southern blots performed as previously described (Luo et al., 1995; Miao et al., 2000). RNA extraction and Northern blots were performed as previously described (Rountree and Selker, 1997).

2.3. Analysis of PARP, MacroD and zf-PARP sequences

Fungal PARP-like proteins, MacroD-like, zf-PARP-like and their ORFs were identified using the BLASTP and TBLASTN programs at NCBI (http://www.ncbi.nih.gov). The BLASTP program was also used at the Broad Neurospora Genome Project database (http://www.broad.mit.edu/annotation/genome/neurospora) to identify the NPO and MacroD proteins, and the NGP genome browser was used to identify their ORFs. Protein motifs and domains were verified in the SMART database (http://www.smart.embl-heidelberg.de/). All sequence alignments and analysis was performed with programs at the SDSC Biology Workbench. The BL2SEQ program was used to compare NPO with human PARP-1 and PARP-2. The *npo* gene and amino acid sequence shown in Fig. 3 was generated with the Publish program using Genetics Computer Group (GCG) software.

2.4. Analysis of subcellular localization of GFP tagged proteins

PCR products of the *hp1*, *rap1*, *mcd* (MacroD) and *npo* genes amplified from wild type Neurospora were cloned into *pMF272* (Honda and Selker, 2009) to allow *his-3* targeting of GFP tagged fusions expressed from the Neurospora *ccg-1* promoter. These PCR products spanned the start and stop codons of these genes, excluding 5′ and 3′ UTR sequences. The details of all cloning steps are available upon request. The Neurospora *yph1* and *zfp* (zf-PARP) genes were cloned, along with 2 kb of upstream sequences, as *NotI–PacI* PCR fragments into *NotI–PacI* digested *pMF272*. The *NotI–PacI* *pMF272* restriction fragment lacks the *ccg-1* promoter. All GFP fusion constructs were used to transform a *his-3* targeting strain p49 (relevant genotype: *his-3*; *inl*; *npo*$^{+}$) obtained by crossing the original *npo* KO strain (14-6-1-1A) with FGSC 7508. Conidia from transformants were imaged using a Zeiss LSM 510 confocal microscope at 630× magnification. Images were taken

Please cite this article in press as: Kothe, G.O., et al. PARP is involved in replicative aging in *Neurospora crassa*. Fungal Genet. Biol. (2010), doi:10.1016/j.fgb.2009.12.012

as Z-sections and analyzed using the program ImageJ. Individual slices were selected and saved as JPEGs.

2.5. Knockout of npo by homologous replacement

The *npo* gene was amplified by PCR from wild type *N. crassa* using the following primers: 5′-CAAATGGACGAAAGAGGAGA-3′ and 5′-TGGTGAAAGCAAGGATGGAA-3′. The 6.5 kb PCR product was digested with *Eco*RI and *Sac*I, and cloned into pBluescript SK+. This construct was then digested with *Xho*I to remove the *npo* ORF and the hygromycin B-resistant gene (*hph*), derived from pCB1003 (Carroll et al., 1994), was cloned in its place. The resulting plasmid (pP1) contains the *hph* gene flanked by 1.9 kb and 1.0 kb of *npo* upstream and downstream sequences, respectively. To knockout the *npo* gene, wild type *N. crassa* (74-OR31-14a) was transformed with an *Eco*RI–*Sac*I fragment from pP1. Transformation was carried out by electroporation as described (Ninomiya et al., 2004) and hygromycin resistant transformants were crossed to a wild type *N. crassa* strain of opposite mating type (74-OR31-16A) to render the integrations homozygous. Finally, *npo* knockout mutants were identified by PCR and Southern hybridization.

2.6. Cloning and mutation of npo by RIP

npo was cloned by PCR amplification from wild type *N. crassa* (N150, 74-OR23-IVA) using the following primers: (2653F) 5′-TCGAATTCATGCCGCCCAGACGAGCAAAG-3′; (2653R) 5′-CTGCGGCCGCTCATACGCAATGTACTCGTTG-3′. The PCR product was digested with *Eco*RI and *Not*I and cloned into *pBM61* (Margolin et al., 1997) to generate *pGK111*. This construct was linearized with *Dra*I, and targeted to the *his-3* locus in strain N1674. Ten transformants were isolated, and correct integrations were confirmed by Southern hybridization. Four of the transformants (pGK111-T1, T2, T3, T4) were crossed with strain N1444 and DNAs from 10 histidine prototrophic progeny from each of the four crosses were analyzed for evidence of mutation of *npo*. Probing of Southern blots of *Dpn*II/*Sau*3A digested DNAs with *npo* sequences revealed RFLPs and heavy methylation in progeny 11 (P11), among others. P11 was obtained from a cross of strain pGK111-T2 with N1444. From here on this strain is referred to as N3180. The endogenous *npo* gene was cloned by PCR from strain N3180 using the following primers: (2653F2) 5′-CTTCACACACTTCACACCTTTGTTTC-3′; (2653R2) 5′-GCTATCTTGACACGGAAAAG-3′. Digestion of the PCR product with *Dpn*II confirmed the presence of the RFLPs detected by Southern blot, and the PCR product was gel isolated and sent for sequencing using primer 2653F. The *npo* allele present in N3180 is designated npo^{RIP1} (see Table 1).

2.7. Testing for genetic interactions between npo^{RIP1} and N. crassa Sirtuins (nsts)

For the purpose of isolating the npo^{RIP1} allele in a *mat a* background, and to look for possible genetic interaction between *npo* and *nst-1*, N3180 was crossed with N1983 (*mat a; mtr col4; nst-*1^{RIP1} *trp-2*). No obvious defects in growth or development were observed in double mutant progeny. Strain N3181 (*mat a*; npo^{RIP1}; *nst-*1^{+}) was obtained from this cross. To isolate npo^{RIP1} in a background with a TPE marker and both *nst-1* and *nst-3* mutations, N3181 was crossed with N2636 (*mat A nst-*3^{RIP1}; *mtr col4*; *telVR::hph::T*; *nst-*1^{RIP1} *trp-2*). Numerous progeny were isolated from this cross and Southern blots were used to determine their genotypes. Among the progeny were P6 (*nst-*3^{+}; npo^{+} *telVR::hph::T*; *nst-*1^{+}), P80 (*nst-*3^{+}; npo^{RIP1} *telVR::hph::T*; *nst-*1^{+}) and P23 (*nst-*3^{RIP1}; npo^{+} *telVR::hph::T*; *nst-*1^{+}) which were tested for TPE (see Fig. 7) along with others. No obvious defects in growth or development were observed for triple mutant progeny.

Table 1
Neurospora crassa strains used in this study.

Strain number	Genotype	Source
N150	*mat A*	FGSC 2489
N1444	*mat a his-3;* am^{132}	This study
N1674	*mat A his-3; lys-1* am^{132} *inl;* am^{RIP}*::hph::*am^{RIP}	Hays et al. (2002)
N1983	*mat a; mtr col4;* $nst\text{-}1^{RIP1}$ *trp-2*	This study
N2636	*mat A* $nst\text{-}3^{RIP1}$*; mtr col-4; telVR::hph::T;* $nst\text{-}1^{RIP1}$ *trp-2*	Smith et al. (2008)
N3180	*mat A his-3::*npo^{RIP0}*;* am^{132} npo^{RIP1}	This study
N3181	*mat a;* npo^{RIP1}	This study
74-OR31-16A	*mat A al-2; pan-2;cot-1*	de Serres (1980)
74-OR31-14a	*mat a al-2; pan-2; cot-1*	de Serres (1980)
MKI-1411A	*mat A al-2; pan-2; cot-1; npoKO*	This study
MKI-1414a	*mat a al-2; pan-2; cot-1; npoKO*	This study
14-6-1-1A	*mat A al-2; pan-2; cot-1; npoKO*	This study
G1	*mat A his-3 cyh-1 al-1; mtr; inl*	FGSC 7508
P49	*mat A his-3 cyh-1 al-1; inl*	This study

2.8. TPE assays

Progeny from the cross of N3181 with N2636 were spot-tested on hygromycin to assay the effects of mutation of *npo*, *nst-1* and *nst-3* on TPE in genetic backgrounds with *telVR::hph::T* (Smith et al., 2008). All possible combinations of alleles were analyzed. Approximately 1000 conidia were spot-tested on FGS plates containing 600 μg/ml or 1.5 mg/ml hygromycin and supplemented with alanine, lysine, inositol and anthranillic acid. Spot-tests were also done on identical plates with no hygromycin as a control for growth.

2.9. Mutagen sensitivity assays

For mutagen sensitivity assays, progeny from the cross of N3181 with N2636 were spot-tested on the same media used in the TPE assays, but containing either MMS (0.03%), MNNG (0.5 μg/ml), EMS (0.3%) or CPT (0.3 μg/ml). As with the TPE assay approximately 1000 conidia were spot-tested, and identical control plates with no mutagen were used as a control for growth. Mutagen sensitivity of the *npo* KO strain was tested as previously described (Watanabe et al., 1997).

2.10. PARylation assay

Crude *N. crassa* extracts were incubated in 50 mM Tris–HCl (pH 8.0), 10 mM $MgCl_2$, 1 mM dithiothreitol, 10 μM (74 KBq/nmol) ^{32}P-NAD (Du Pont), 20 μg/ml activated DNA (Sigma) and 20 μg/ml calf thymus type II-A histones (Sigma H9250) at 25 °C for 30 min. To stop the reaction, the PARP inhibitor 3-aminobenzamide was added to 5 mM and unincorporated NAD was removed using spin columns containing Sephadex G-50 resin (GE Healthcare). *Escherichia coli* extracts expressing human recombinant PARP-1 (Ikejima et al., 1990) were used as positive controls. After centrifugation at 300g for 4 min, the eluent containing ^{32}P-PARylated proteins was treated with 0.1 M NaOH at 37 °C for 30 min to detach ^{32}P-PAR, and the solution was neutralized by addition of Tris–HCl (pH 7.5) to 50 mM and HCl to 0.1 N. After extraction with water-saturated phenol and chloroform–isoamyl alcohol (49:1 (v/v)), ammonium acetate was added to 2 M and ^{32}P-PAR was ethanol-precipitated. After washing with 70% ethanol, the fraction was dried and dissolved in a loading dye containing urea (Panzeter and Althaus, 1990). The fraction was then analyzed by 20% polyacrylamide gel electrophoresis as described elsewhere (Panzeter and Althaus,

Please cite this article in press as: Kothe, G.O., et al. PARP is involved in replicative aging in *Neurospora crassa*. Fungal Genet. Biol. (2010), doi:10.1016/j.fgb.2009.12.012

1990). The gel was exposed and analyzed with BAS2500 (Fuji Film). The radioactive area containing ^{32}P-PAR was cut out and further analyzed. The gel fragments were rinsed with water and crushed. The radioactive material was eluted and digested by incubation overnight at 25 °C in 100 µl of a PARG buffer containing 20 mM potassium phosphate (pH 7.5), 10 mM β-mercaptoethanol, 0.05% Triton X-100 (Sigma), 0.1% bovine serum albumin and rat PARG-conjugated with glutathione-*S*-transferase (GST-PARG) (Shimokawa et al., 1999). Treatment with GST-PARG digested PAR to ADP-ribose, and the reaction mixture was treated with perchloric acid at 0.5 N on ice for 20 min and neutralized with 0.7 M glycyl-glycine-3 M potassium hydroxide and centrifuged at 15,000g for 5 min at 4 °C. The supernatant was subjected to high performance liquid chromatography (HPLC). HPLC was carried out using Develosil columns (C30-UG-5, Ø46X250 mm, Nomura Chemicals). UV absorbance was monitored at 254 nm (Toso, UV-8000). A linear gradient elution for 100 min using buffer A (0.1 M ammonium acetate) and buffer B (50 mM ammonium acetate–50% acetonitrile) was performed, ranging from 2% to 100% buffer B at a flow rate of 0.5 ml/min. The retention time of ADP-ribose was 17–19 min. Each 0.5 ml fraction between 13 and 20 min was concentrated and spotted on DE81 paper (Whatman) and analyzed by BAS2500.

2.11. Telomere erosion assay

Genomic DNAs from wild type and the *npo* strain were digested with *Cla*I and *Hin*dIII. Electrophoresis was carried out in a 2.5% agarose gel for 5 h at 50 mV and Southern blots performed as previously described (Luo et al., 1995; Miao et al., 2000). These blots were then probed with a non-isotopically labeled oligo composed of seven direct tandem copies of the telomere repeat sequence [5′-CCCTAA-3′].

3. Results and discussion

3.1. There are two classes of fungal PARP-like proteins

Semighini et al. (2006) observed that PARP homologs exist in fungi that have multicellular hyphae and sophisticated developmental structures, but lack a prominent yeast-like budding growth phase. The canonical PARP enzyme from mammals, PARP-1, contains an N-terminal zinc finger DNA-binding domain (zf-PARP), a BRCT motif that is the major target for auto-modification, a WGR motif, and a core catalytic domain (Ame et al., 2004; Kim et al., 2005). We performed TBLASTN searches through the NCBI (http://www.ncbi.nih.gov) fungal genome databases using the human PARP-1 catalytic domain as the query. We then analyzed the hits using the SMART database (http://www.smart.embl-heidelberg.de/) to confirm the presence of a PARP catalytic domain (pfam 00644). Our analysis revealed two classes of PARP-like proteins: (1) Homologous to *A. nidulans* PrpA, containing BRCT (pfam 00533) and WGR motifs (pfam 05406) and (2) those with a catalytic domain most similar to mammalian PARP-6/PARP-8 family members and having a carboxyl terminal extension showing homology to the catalytic domain (SMART 00212) of ubiquitin-conjugating enzyme E2 (Fig. 1A). This domain organization seems to be specific to filamentous fungi. We refer to this second class of fungal PARP-like proteins as PARP/E2. Like the PrpA class, the PARP/E2 proteins are broadly distributed in the euascomycetes. In fact, *N. crassa* is the only euascomycete represented in the NCBI fungal genome databases (25 species) that does not have a PARP/E2 homolog, raising the possibility that a *N. crassa* homolog is in a sequencing gap. Homologs in the PARP/E2 class were also found in the basidomycetes *Coprinus cinereus* (EAU83704.1) and *Phanerochaete chrysosporium* (unannotated protein, contig accession: AADS01000086, gi:46851846, approx. coordinates 71,000–75,000).

3.2. N. crassa has a single PARP homolog of the PrpA class

Fungal PARP proteins of the PrpA class lack an amino terminal zinc finger DNA-binding domain (zf-PARP), but have both an N-terminal BRCT motif and a WGR motif (Semighini et al., 2006). A BLASTP search with PARP-1 sequences through the Broad Institute Neurospora genome database (http://www.broad.mit.edu/annotation/genome/neurospora) identified a single ORF encoding a predicted protein of 592 amino acids with a WGR motif, but lacking a BRCT motif (NCU08852.3, EAA31746, GI:157070000, accession AABX02000063.1). We feel that the most likely start codon for this ORF is 235 nucleotides upstream of that suggested by the Broad annotation, which would predict a protein of 670 amino acids with

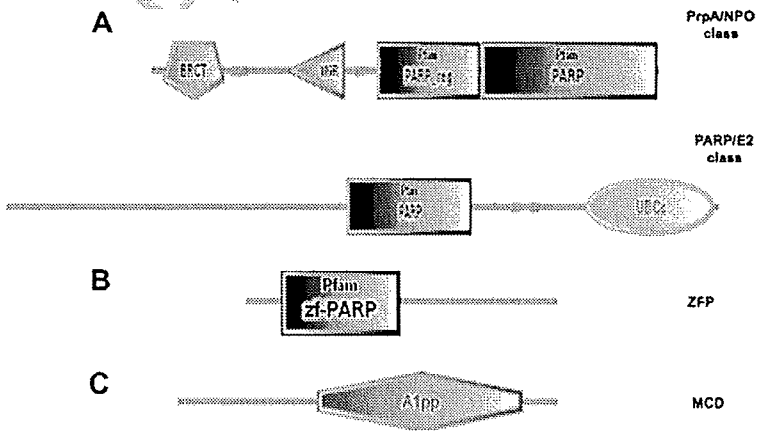

Fig. 1. Domain organization of fungal PARP-like proteins and associated DNA and PAR binding proteins. (A) Schematic representation of the domain organization of the two classes of fungal PARP proteins. The complete amino acid sequences of NPO. *Neurospora crassa* PARP ortholog [CAD21266] and *Aspergillus nidulans* AN0482.2 [XM_652294.1] were used as queries to search the SMART database (smart.embl-heidelberg.de). Searching with NPO identified BRCT [IPR001357], WGR [IPR008893], PARP-regulatory [PF02877], and PARP-catalytic [PF00644] domains, defining the PrpA/NPO class. Searching with AN0482.2 identified PARP-catalytic [PF00644] and Ubiquitin-conjugating enzyme E2 catalytic domains [SM00212], defining the PARP/E2 class. (B) Domain organization of the Neurospora MacroD protein. The complete amino acid sequence encoded by Neurospora ORF NCU07925.3 was used to search the SMART database indentifying the A1 pp domain [SM00506]. (C) Domain organization of the Neurospora zf-PARP protein. The complete amino acid sequence of a Neurospora hypothetical protein [Broad coordinates LGI, containing 2:447973 – 449833+] was used to search the SMART database identifying a single zf-PARP Pfam domain [PF00645].

Please cite this article in press as: Kothe, G.O., et al. PARP is involved in replicative aging in *Neurospora crassa*. Fungal Genet. Biol. (2010), doi:10.1016/j.fgb.2009.12.012

both WGR and BRCT motifs, as expected for a member of the PrpA class (Fig. 1A). We refer to this protein as Neurospora PARP Ortholog (NPO). The presence of BRCT motifs in the PrpA class of fungal PARPs, and their absence from PARP-2 homologs, suggests that proteins of the PrpA class are more closely related to PARP-1. However, comparison of NPO with human PARP-1 and PARP-2 using the BL2SEQ program suggests a closer relationship with PARP-2 [NPO:-PARP-1, $e = 10^{-79}$, identities = 216/681 (31%), similarities = 335/681 (49%), gaps = 67/681 (9%); NPO:PARP-2, $e = 3 \times 10^{-82}$, identities = 187/464 (40%), similarities = 259/464 (55%), gaps = 39/464 (8%)]. In agreement with our analysis Semighini et al. (2006) observed that PrpA-like PARPs belong to a microbial clade more similar to PARP-2 than PARP-1.

3.3. Fungal zf-PARP proteins, macro domain proteins and nuclear localization of NPO

Fungal PARP-like proteins, including NPO, lack any obvious DNA-binding domain, raising the question of whether these proteins are principally associated with chromatin, like their metazoan counterparts. NPO might contain a cryptic DNA-binding domain or could require a partner for DNA binding. Because PARP-1 contains a highly characteristic amino terminal zinc finger DNA-binding domain (zf-PARP), we sought to identify fungal proteins containing a similar motif. To this end we performed TBLASTN searches through the NCBI fungal genome database using the PARP-1 zinc finger as query. These searches identified a single Neurospora ORF encoding a protein of 404 amino acids, containing a single zinc finger of the zf-PARP class (Fig. 1B). We refer to this protein as ZFP. Although this ORF has not been annotated with an NCU number in the Broad database, we believe that it represents a functional gene, as a GFP tagged form, expressed via its own promoter, has a punctate nuclear staining pattern, similar to the heterochromatin associated protein, HP1 (Fig. 2) (Freitag et al., 2004a). To determine the subcellular location of NPO we tagged the protein with GFP at its carboxyl terminus, and expressed the fusion protein in aerial hyphae and conidia using the developmentally regulated *ccg-1* promoter (Fig. 2) (Freitag et al., 2004b; Loros et al., 1989; McNally and Free, 1988). GFP tagging of ectopically expressed NPO verifies that this protein is also localized primarily to nuclei (Fig. 2), and thus has a functional nuclear localization signal. The subnuclear distribution of NPO seems to be essentially uniform, in comparison to proteins localized specifically to heterochromatin (HP1), telomeres (RAP1) and rDNA (YPH1) (Fig. 2).

We have not been able to identify any PARG-like protein in any filamentous fungal database, and thus PAR may be a more stable posttranslational modification in fungi than in higher eukaryotes. Although we were unable to identify fungal proteins with the PAR-binding C2H2 zinc finger (PBZ) domain (Ahel et al., 2008), we did identified one ORF encoding a protein of 277 amino acids with a single Macrodomain (also designated as A1 pp) (Fig. 1C). Macrodomains have also been shown to bind PAR both *in vivo* and *in vitro* (Karras et al., 2005). The Neurospora Macrodomain protein is annotated in the Broad database as NCU07925.3, and we refer to it as Macrodomain (MCD). An over-expressed GFP tagged form of MCD has essentially uniform cytoplasmic and nuclear distributions, but is slightly more concentrated in nuclei than in cytoplasm (Fig. 2). Thus, while NPO has an autonomous nuclear localization signal, it may be brought to DNA via association with other proteins such as ZFP. Furthermore, while fungi are unlikely to remove PAR via a glycohydrolase activity, as mammals do, they are likely to recognize PAR via nuclear localized Macrodomain proteins such as MCD.

3.4. npo is a nonessential gene in N. crassa

After verifying the nuclear distribution of NPO we then isolated *N. crassa* stains with mutations in the *npo* gene using Repeat Induced Point mutation (RIP) (Selker, 1990) and made knockout strains by replacing the *npo* coding sequence with the bacterial hygromycin phosphotransferase gene (*hph*) (Figs. 3 and 4A and B). Both homozygous and heterozygous crosses of strains carrying duplications of *npo* at the *his-3* locus were fully fertile. These results suggest that *npo* is not required in the brief diploid phase for completion of meiosis, as heterozygous duplications would be expected to trigger meiotic silencing by unpaired DNA (MSUD) (Aramayo and Metzenberg, 1996; Shiu et al., 2001). However, it is also possible that there is enough transcript or protein present in ascogenous hyphae to override the effect of MSUD during the diploid phase.

We confirmed the presence of mutations by RIP in progeny from these crosses by Southern hybridization and DNA sequencing. Clear evidence of RIP was detected by Southern hybridization in 6 out of 40 progeny. None of the six progeny exhibited any gross morphological or developmental phenotypes. Sequencing

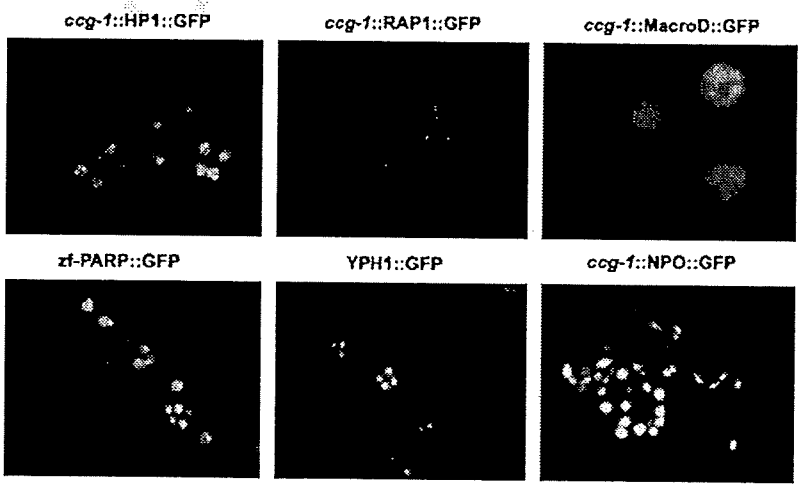

Fig. 2. Confocal images of GFP-tagged Neurospora proteins. Expression of heterochromatin protein 1 (HP1::GFP), a telomere repeat binding protein (RAP1::GFP), MacroD::GFP and NPO::GFP was driven by the *ccg-1* promoter. An rDNA associated protein (YPH1::GFP) and zf-PARP::GFP were expressed via their endogenous promoters.

Please cite this article in press as: Kothe, G.O., et al. PARP is involved in replicative aging in *Neurospora crassa*. Fungal Genet. Biol. (2010), doi:10.1016/j.fgb.2009.12.012

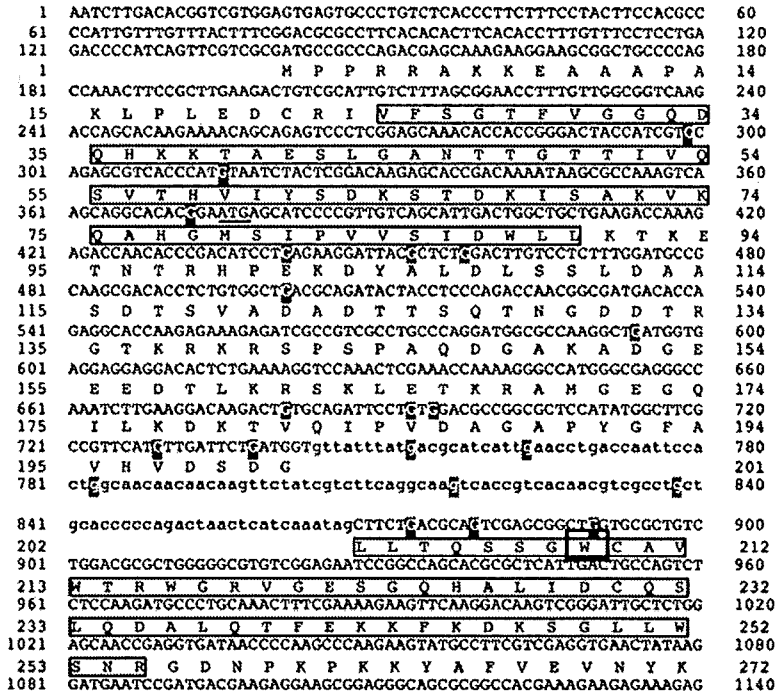

Fig. 3. Sequence of the *npo*^{RIPF} allele. The NPO protein sequence is indicated beneath the upper case nucleotide coding sequence. Lower case nucleotides represent intron sequences. The boxed amino *acid* in the first exon indicate the BRCT domain and the boxed amino acids in the second exon indicate the WGR motif. Guanine residues mutated to adenines are highlighted, and the tryptophan codon that was mutated to a stop codon is boxed. The sequence of the *npo*^{RPI} allele had been deposited in Genbank with the accession number EU869543.

of a PCR product amplified from progeny number 11 (P11) identified 21 C:G to T:A transition mutations in a 591 base pair segment of the endogenous *npo* gene (Fig. 2). All G to A mutations were found on the coding strand, spanning the first and second exons. The 21 mutations affected 15 codons, with five mutations occurring in the intron. Of the 16 mutation occurring in codons, four were in 3rd position and silent (V53, L106, L203 and Q205), seven were in 1st position, resulting in conservative substitutions (V59 → I, E101 → K, D121 → N, D152 → N, V181 → M, V197 → I and D200 → N), two were in 1st position resulting in nonconservative substitutions (G78 → R and A105 → T) and one was in second position producing a stop codon (W209 → stop). The conservative substitution at position 185 (V185 → I) resulted from G to A transitions in both the 1st and 3rd positions. The introduction of a stop codon at W209 is very likely to eliminate NPO function, as it occurs in the amino terminal region of the WGR motif, upstream of the PARP catalytic domain (Fig. 3). We refer to this allele as *npo*^{RIP1} and the original progeny harboring the allele (P11) as N3180.

All tested strains carrying *npo*^{RIP1} were fully fertile as males or females, and homozygous crosses appeared normal as well. Knockouts of *npo* were made by homologous replacement of the *npo* coding region with *hph* in a wild type background. Proper replacements were confirmed by PCR analysis and Southern blots (Fig. 4A and B). Strains with the *npo* KO, like strains with the *npo*^{RIP1} allele, did not exhibit gross morphological or developmental phenotypes, and were fully fertile in heterozygous and homozygous crosses. We conclude that *npo* is a nonessential gene in *N. crassa* and is not required for normal growth or development. These results stand in contrast to what was reported for a *prpA* knockout in Aspergillus, which was lethal in haploid strains, and produced severe growth restrictions and developmental phenotypes in heterozygous diploid strains (Δ*prpA*/+), described as haplo-insufficient (Semighini et al., 2006).

3.5. NPO is a PAR-polymerase

We assayed PARylation activity in extracts from both wild type and *npo* KO strains to determine if NPO functions as a protein PAR-polymerase. To our knowledge, results from PARylation assays have only been reported for mammalian systems. To assay PARylation, crude extracts from wild type and the *npo* KO strain were prepared from conidia that had either been treated or not treated with MMS for 60 min. The crude extracts were incubated with ^{32}P-NAD, sheared DNA and histones. As a positive control, an assay was also performed on extracts from *E. coli* cells expressing recombinant human PARP-1. PAR was detached from proteins by alkaline treatment and analyzed on 20% PAGE. As shown in Fig. 5A, the MMS-treated wild type strain produced a PAR-ladder like the human PARP-1 control (right-most lane), but the *npo* KO strain did not. To confirm that the ladder observed with the MMS-treated wild type strain reflected PAR, the radioactive material was eluted from the gel, digested with PAR-glycohydrolase (PARG), which specifically cleaves PAR into ADP-ribose, and analyzed by HPLC. As shown in Fig. 5B, the radioactivity that eluted at the retention time of ADP-ribose, namely at 18–19 min, is higher in the PARG-treated sample than in the untreated control. It is possible that the radioactivity detected at 18–19 min in the PARG untreated control is due to degradation of PAR to ADP-ribose during PARG-treatment or due to unrelated products generated during the ^{32}P-NAD incorporation reaction. The control extract containing human PARP-1 also showed high intensity spots at 18–19 min, corresponding to ADP-ribose. We conclude that *N. crassa* PARylation increases in response to MMS treatment, and that this activity depends on NPO, which is likely responsible for most or all PARylation in *N. crassa*.

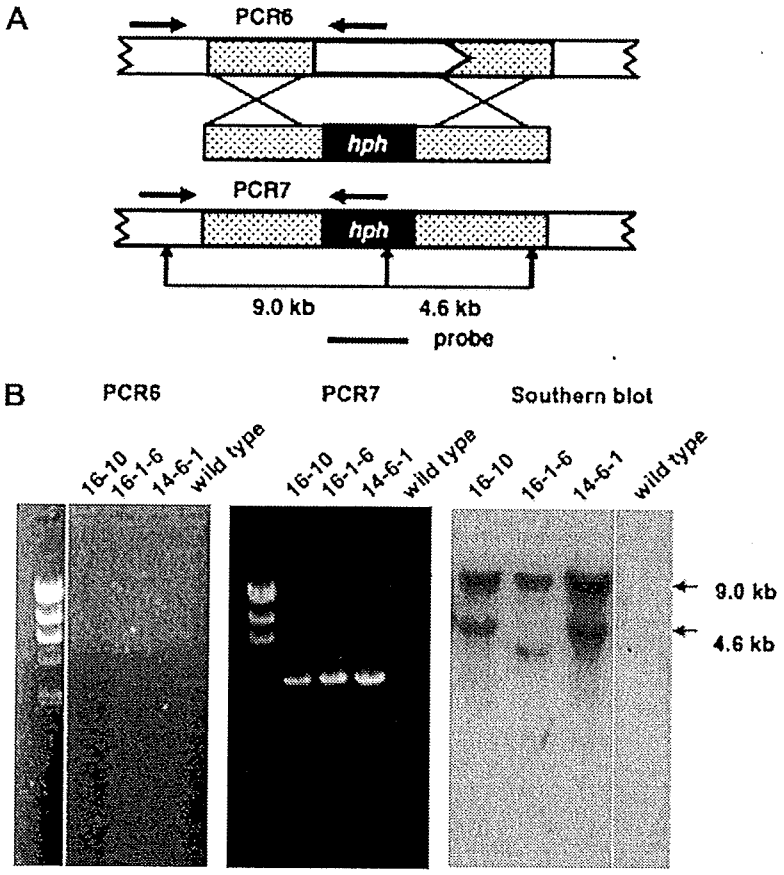

Fig. 4. Disruption of the *N. crassa npo* gene by homologous recombination. (A) Schematic illustration of knockout strategy for the *npo* gene. A white arrow box represents the *nop* gene and shows the direction of transcription. Stippled boxes indicate immediate flanking sequences. The knockout construct is shown below the genomic sequence with the *E. coli hph* gene represented by a black box. The genomic sequence resulting from correct replacement is shown beneath the knockout construct. Horizontal black arrows indicate the positions of PCR primers used to analyze the transformants. Vertical black arrows indicate restriction sites used to characterize the transformants by Southern hybridization. A horizontal black line represents the probe used int he Southern blot. (B) The images labeled PCR6 and PCR7 are ethidium bromide-stained agarose gels with size markers run in the left-most lanes. The next three lanes contained PCR products that had been amplified from wild type *N. crassa* DNA, as controls. The position of primers for the PCR6 and PCR7 reactions are shown in panel A. The right-most image shows an autoradiograph of a Southern blot probed with *hph* sequences. DNAs from the indicated transformants were digested with *Nco*I. DNA from wild type *N. crasse* was run in the right-most lane as a control.

3.6. npo transcription is induced by MMS treatment

It is well established that auto-modification of mammalian PARP-1 increases dramatically with the binding of the protein to double and single-strand DNA breaks. Although the transcriptional response of the mammalian PARP-1 gene to DNA damaging agents has not been reported, plant PARP-1 and PARP-2 gene transcription is highly induced by DNA damage (Doucet-Chabeaud et al., 2001). In addition, Semighini et al. (2006) found *prpA* steady-state transcript levels increased in response to MMS, BLM and 4-NQO treatments. Our results from PARylation assays demonstrated a dramatic increase in NPO activity in response to MMS treatment. To determine if this reflected a change in *npo* transcript levels or enzyme activity, we performed Northern blots of RNAs isolated from wild type and *npo* KO strains that had either been treated or not treated with MMS. The blots were probed with *npo* sequences, and *cox-5* sequences as a control for the loading. In untreated wild type cells, *npo* transcripts were undetectable by Northern blot, but a large accumulation of *npo* transcript was detected 30 min after treatment of wild type cells with MMS, and high levels of transcript were still detectable 120 min after treatment (Fig. 6). As expected, no *npo* transcripts were detectable in the *npo* KO strain (Fig. 6). Thus *npo* transcription is likely to be regulated in response to DNA damage, like the *A. nidulans prpA* gene.

3.7. npo mutant strains are not sensitive to DNA damaging agents

Genetic and biochemical studies of mammals established roles for PARP-1 in DNA repair and genome stability (Masutani et al., 2003; Watanabe et al., 2004). The fact that the steady-state transcript levels of *npo* were regulated by exposure to MMS suggested that NPO may play a role in a DNA damage response. We tested the effects of a number of DNA damaging agents on *N. crassa* strains carrying either the npo^{RIP1} allele or the *npo* KO. We tested CPT, EMS, H_2O_2, HU, MMS, MNNG and UV (Fig. 7), as well as BLM (data not shown). Neither mutant showed sensitivity to any of these compounds. Semighini et al. (2006) found the haplo-insufficient Δ*prpA*/+ mutant to be extremely sensitive to both phleomycin (PLM), which induces double-strand breaks, and the UV-mimetic agent 4-NQO. While we did not test PLM, the *npo* mutants were not sensitive to BLM, which also induces DNA double-strand breaks (Povirk et al., 1977). Because *npo* transcript levels increase in response to MMS, it is likely that NPO function is connected with a DNA damage response. The fact that *npo* mutants are not sensitive to DNA damaging agents suggests the function may be redundant, or it may impact a nonessential aspect of repair. Alternatively, NPO may function in related processes such as regulating expression of genes controlled by DNA damage. The fact that *A. nidulans* PrpA is necessary for normal repair reveals divergence

Please cite this article in press as: Kothe, G.O., et al. PARP is involved in replicative aging in *Neurospora crassa*. Fungal Genet. Biol. (2010), doi:10.1016/j.fgb.2009.12.012

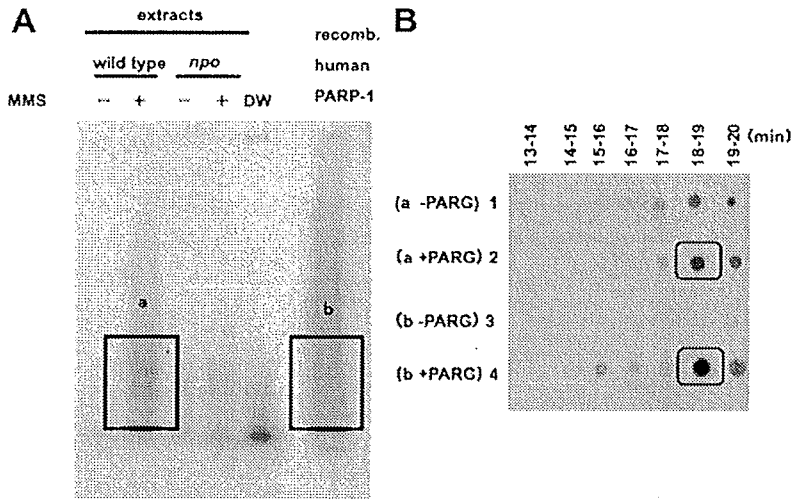

Fig. 5. Verification of NPO PARylation activity. (A) Autiradiogram of a 20% poly acrylamide gel showing ^{32}p-PAR ladder. PARylation reactions with extracts from wild type *N. crassa* cells treated (+) or not treated (−) with MMS were run alongside reactions with extracts from *npo* KO cells treated (+) or not treated (−) with MMS. The lane labeled DW is a negative control reaction using distilled water in place of extract. The right-most lane contains a positive control reaction with recombinant human PARP-1 expressed in *E. coli*. The boxed regions labeled a and b were excised and the radioactivity was eluted fir analysis by HPLC. (B) An autoradiogram (BAS2500) of fractions from HPLC blotted onto DE81 paper (Whatman) with retention times indicated above and sample designations on the left. Eluents of ^{32}p-PAR from these gel slices were either treated with recombinant PARG, or not, and fractionated by HPLC as described in Section 2. The boxed regions show the peak signals eluted at the retention time for ADP-ribose.

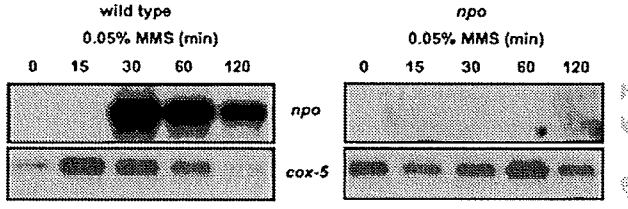

Fig. 6. Analysis of *npo* transcription by Northern blot. The left panel shows an autoradiogram of a northern blot of RNAs extracted from wild type *N. crassa* after the indicated duration of MMS treatment. The upper panel shows results of probing the blot with *npo* sequences and in the lower panel shows results of probing with *cox-5* sequences ad a control for loading. The right panel shows the same for the *npo* strain.

in DNA damage response pathways between Neurospora and Aspergillus.

3.8. NPO is not a global regulator of TPE

In metazoans, PARP enzymes are involved in chromatin-mediated regulation of transcription (Krishnakumar et al., 2008). Although considerable progress has been made in understanding the role of PARPs in regulating chromatin structure, simple genetic studies to test their possible involvement in epigenetic position effects, such as Telomere Position Effect (TPE), are lacking. We recently developed *N. crassa* strains with markers at subtelomeric positions to examine TPE (Smith et al., 2008). This system allowed us to identify factors that control TPE, including several Sirtuins, termed Neurospora Sirtuins (NSTs). To analyze the effect of mutations in *npo* on TPE, we crossed the *npo*^{RIP11} allele into a background with the *E. coli hph* gene targeted to telomere VR (*telVR::hph::T*). We found significant derepression of *hph* at telomere VR in a strain with mutations in the *N. crassa* Sirtuin gene *nst-3* (*nst-3*^{RIP1}), but not in a strain with *npo*^{RIP1} (Fig. 8).

3.9. NPO is not involved in DNA methylation or DNA methylation-dependent silencing

In mammals it has been reported that PARP-1 is antagonistic to DNA methylation. Treatment of mouse fibroblasts with the competitive PARP inhibitor 3-aminobenzamide (3-AB) resulted in DNA hypermethylation and PAR has been shown to inhibit the activity of the maintenance DNA methylase, DNMT1 (Reale et al., 2005). *N. crassa* is the simplest genetically tractable system used to study DNA methylation. In *N. crassa* virtually all DNA methylation occurs in transposons that have been mutated by RIP (Selker et al., 2003) and this methylation is not confined to symmetrical positions (Selker et al., 1993). Numerous viable *N. crassa* mutants with reduced methylation have been described, including *dim-2*,

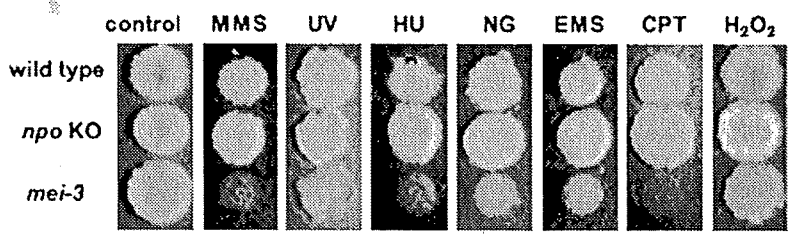

Fig. 7. Mutagen sensitivity of the *npo* KO strain. Spot-tests of conidia on FGS plates for wild type *N. crassa* (top), the *npo* (middle) and *mel-3* strains (bottom) were done as described in Section 2. The *mei-3* strain was used as a positive control for mutagen sensitivity. Panels from left to right are as follows: no mutagen;0.015% methyl methane sulfonate(MMS); conidia pretreated with 450 J/MF UV; 30 mM hydroxy urea (HU); 0.05 μg/ml N-methyl-N′-nitro-N-nirtosoguanidine (MNNG);0.3% ethyl mithane sulfonate (EMS); 0.3 μg/ml camptothecin (CPT) and 0.0015% H_2O_2.

Please cite this article in press as: Kothe, G.O., et al. PARP is involved in replicative aging in *Neurospora crassa*. Fungal Genet. Biol. (2010), doi:10.1016/j.fgb.2009.12.012

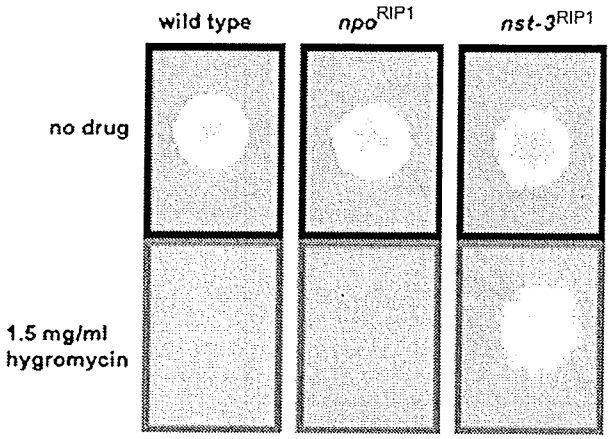

Fig. 8. Telomere position effect assay. Spot-tests of conidia on FGS plates for wild type *N. crassa*, *npo*^{RIP1}, and *nst-3*^{RIP1} strains on media with 1.5 mg/ml hygromycin or no hygromycin, as described in Section 2.

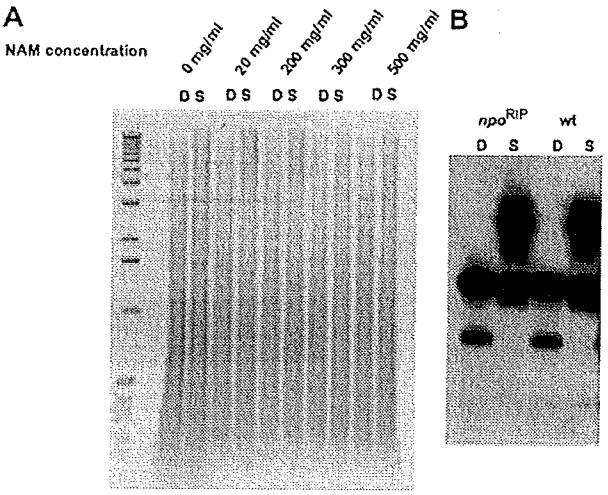

Fig. 9. Absence of effects of NAM treatment and npo mutation on DNA methylation. (A) Approximately 1 μg samples of chromosomal DNA, isolated from wild type *N. crassa* (N150) grown for 3 days in Vogles minimal media with the indicated concentrations of NAM, where digested either with *Dpn*II (D) or Sau3A(S) and fractionated on a 1X TAE/0.8% agarose gel containing 1 μg/ml ethidium bromide. The left-most lane contains 0.5 μg of 1 kb DNA ladder (invitrogen). (B) A Southern blot of chromosomal DNAs from wild type and npo mutant strains digested with *Dpn*II (D) or Sau3A(S), as described for panel A and in Section 2. The Southern blot was probed with ψ63 sequences.

dim-5, and *hpo*. Mutation in any of these genes completely abolishes all detectable DNA methylation (Freitag et al., 2004a; Kouzminova and Selker, 2001; Tamaru and Selker, 2001). Although no mutants with hypermethylation have been described in *N. crassa* thus far, strains of *Ascobolus immersus* carrying silenced copies of the histone H1 gene (*hH1*) were shown to have elevated levels of DNA methylation (Barra et al., 2000). This hypermethylated DNA could be detected globally on ethidium bromide-stained agarose gels, as higher molecular weight fragments after digestion with methylation sensitive restriction enzymes.

As a first test of whether inhibition of NPO effects DNA methylation we treated wild type *N. crassa* cells with high concentrations of nicotinamide (NAM) and looked at global DNA methylation by analyzing *Sau*3A- and *Dpn*II-digested DNAs on agarose gels (Fig. 9A). NAM acts as a strong noncompetitive inhibitor of both Sirtuins and PARPs, and we had previously shown that treatment of *N. crassa* with NAM dramatically reduces silencing of *telVR::hph*, but has no effect on silencing of the methylated transgene *am*^{RIP}*::hph::am*^{RIP} (Smith et al., 2008). No effect on global DNA methylation was observed after NAM treatment (Fig. 9A). The fact that NAM treatment did not relieve silencing of *am*^{RIP}*::hph::am*^{RIP}, suggests that neither NPO nor NSTs are involved in methylation-dependent silencing at this locus. Because it was conceivable that NPO is resistant to NAM, we also tested if mutation of *npo* would affect DNA methylation. Southern blots of *Sau*3A- and *Dpn*II-digested DNAs from progeny with mutations by RIP in the *npo* gene, including strain P11, which is likely to be a null mutant, revealed heavy DNA methylation when probed with *npo* sequences (data not shown). We probed the same Southern blots with Ψ63 sequences, which are normally methylated (Margolin et al., 1998), and did not see any change in DNA methylation at this locus (Fig. 9B). We also looked at global DNA methylation levels by ethidium bromide staining in *N. crassa* strains with the *npo*^{RIP1} allele and saw no effect (data not shown). In addition, presence of the *npo*^{RIP1} allele, or quelling experiments with *npo* sequences, had no effect on silencing of *am*^{RIP}*::hph::am*^{RIP} (data not shown), indicating that NPO is not involved in methylation-dependent silencing. We conclude that *npo* is not involved in DNA methylation.

3.10. The npo knockout causes acceleration of replicative aging

Studies of aging in filamentous fungi have focused largely on replicative aging associated with mitochondrial DNA (mtDNA) rearrangements triggered by mitochondrial plasmid/intron mobilizations (Osiewacz, 2002). Replicative lifespan is a measure of the number of mitotic divisions a cell undergoes before senescence. Analogous to the ERC situation in yeast, these mechanisms seem to be specific to filamentous fungi. Barra et al. (2000) reported that strains of *A. immersus* with silenced copies of the *hH1* gene exhibited a decreased replicative lifespan, along with DNA hypermethylation. Such strains were found to initiate growth normally, but to senesce between 6 and 13 days after germination, whereas strains with unsilenced *hH1* continued with a linear rate of growth for up to 40 days. We observed a similar phenotype for our *npo* KO strain, although the replicative lifespan of *N. crassa* mycelia is considerably longer than that of *A. immersus* (500 days versus 35–40 days, respectively). We grew both wild type and *npo* KO strains on minimal medium in 30 cm race tubes at 34 °C with 12 h dark/light cycles, and were careful to transfer only mycelial fragments upon inoculation (Fig. 10A). The *npo* KO strain had a linear growth rate indistinguishable from wild type for the first 140 days of growth (6 cm/day), at which point the growth rate started to decrease gradually, culminating in senescence at around 300 days (Fig. 10B).

3.11. Telomere erosion does not occur in the npo knockout strain

Eukaryotic microorganisms must maintain telomere length in every proliferating cell type, either by telomerase activity or by recombination. We were therefore interested to test if the increased replicative aging observed in the *npo* strain reflected defective maintenance of telomeres. To determine if mutation of *npo* affects telomere length in *N. crassa*, DNA was isolated from young cultures (~80 h) and old cultures (~8000 h) of both wild type and *npo* KO strains. The DNAs were digested with *Cla*I and *Hin*dIII and Southern blots were probed with telomere repeat sequences. The 8000 h time point was chosen because this is when the *npo* KO strain begins to senesce (Fig. 11A). The Southern blots did not reveal any obvious change in the length of the *npo* KO telomeres, even after 8000 h of culture time (Fig. 11B). Therefore, regulation of telomere length does not appear to be a factor in lifespan reduction for the *npo* KO strain.

Please cite this article in press as: Kothe, G.O., et al. PARP is involved in replicative aging in *Neurospora crassa*. Fungal Genet. Biol. (2010), doi:10.1016/j.fgb.2009.12.012

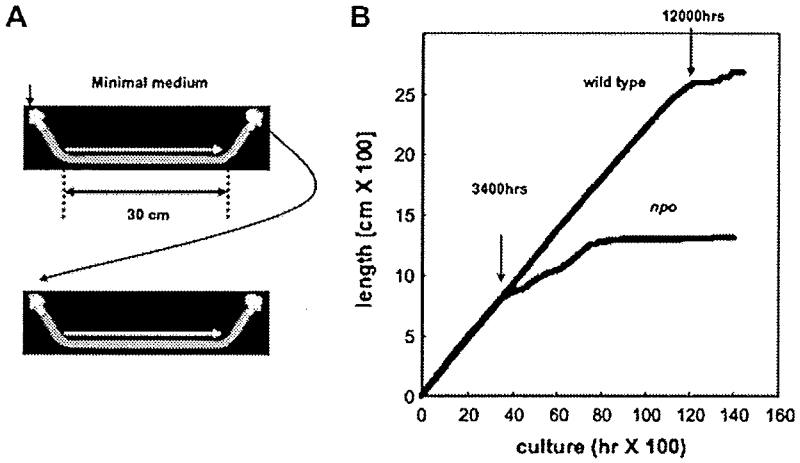

Fig. 10. Method and results of senescence assay. (A) Schematic of race tube strategy for measuring long-term linear extension rate. (B) Plot of growth (cm/h) for wild type *N. crassa* and npo strain. Arrows at 3400 h and 12,000 h indicate entry into senescence for npo and wild type *N. crassa* strains, respectively.

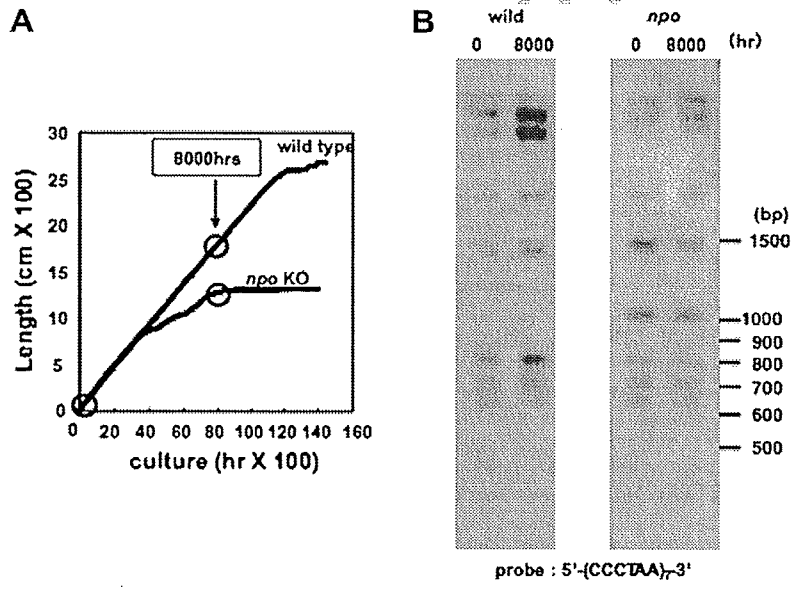

Fig. 11. Telomere stability in wild type and npo mutant strains. (A) Arrows on plot shows time points used in telomere erosion assay. (B) Chromosomal DNAs were isolated from wild type and the npo mutant at the time points indicated in panel A. The DNAs were digested with *Hae*III, blotted as described in Section 2, and probed with telomere repeat sequences.

3.12. PARylation is not universally required for viability or DNA repair

PARP orthologs have been identified in all eukaryotes, excluding yeast. Both plants and animals typically have multiple PARP orthologs, making genetic characterization difficult. Lethality of PARP-1$^{-/-}$/PARP-2$^{-/-}$ mice and evidence linking PARylation with DNA repair and genomic stability support a view that PARylation impacts nuclear functions essential for higher eukaryotic development or survival. Unsuccessful attempts to generate PARP-1/PARP-2 double knockouts in mouse embryonic fibroblasts (Meder et al., 2005) suggest that these functions may be critical for cellular survival. Mutation of dPARP in Drosophila results in larval lethality at the second instar stage, with disruption of heterochromatin organization and elimination of nucleoli (Tulin et al., 2002), again supporting the hypothesis that PARPs provide nuclear functions essential to the cell. Recent work on PARP in the filamentous fungus *A. nidulans* extends this view to PARylating lower eukaryotes (Semighini et al., 2006). Our work in *N. crassa* stands in contrast to what has been found for mammals and *A. nidulans*, as *N. crassa npo* mutants are viable and do not show sensitivity to mutagens, establishing that PARylation is dispensable for both viability and DNA-repair in certain eukaryotes with PARP orthologs. The fact that transcription of PARP genes is induced by DNA damage in both plants (Doucet-Chabeaud et al., 2001) and filamentous fungi (Semighini et al., 2006) does support the idea that there is a universal function for PARylation in DNA repair, but this function may be redundant in *N. crassa*, but not *A. nidulans*.

3.13. PARylation is not required for heterochromatin formation in N. crassa

Two major heterochromatin silencing pathways described in *N. crassa* are TPE (Smith et al., 2008) and cytosine methylation (Selker, 2004). Our analysis indicates that neither pathway is significantly

affected by mutation of *npo*. The histone H3 K9 methylase, DIM-5 (Tamaru and Selker, 2001), and the HP1 ortholog, HPO (Freitag et al., 2004a), are necessary for silencing at all tested *N. crassa* telomeres (Smith et al., 2008), as well as for all detectable DNA methylation. It is formally possible, however, that NPO might regulate TPE at telomeres other than VR or DNA methylation at a subset of unanalyzed genomic loci, although we have no reason to expect this to be so. We have shown that treatment of *N. crassa* with NAM dramatically reduces silencing of *telVR::hph*, but has no effect on silencing of the methylated transgene am^{RIP}::*hph*::am^{RIP}. Before our analysis of the effect of the npo^{RIP1} allele on silencing of *telVR::hph*, we could not fully interpret these data. Our genetic studies now suggest that the mechanism of action of NAM on TPE involves inhibition of NSTs, but not NPO. The fact that NAM treatment did not relieve silencing of am^{RIP}::*hph*::am^{RIP}, strongly suggests that neither NPO nor NSTs are involved in methylation or methylation-dependent silencing at this locus. The observation that PARP-1 activity impacts DNA methylation in mammals implies divergence in pathways that regulate methylation between mammals and filamentous fungi. This is not surprising considering that the activity of DNMT1, which is the primary maintenance methylase in mammals, is inhibited by PAR (Reale et al., 2005). *N. crassa* lacks this form of maintenance methylation, which acts specifically on hemimethylated CpG dinucleotides in conjunction with DNA replication. In *N. crassa*, both maintenance and *de novo* methylation are carried out by a single methyltransferase, DIM-2 (Kouzminova and Selker, 2001), which does not require a symmetrical sequence (Selker et al., 1993). It would be interesting to know whether PARP inhibitors or silencing of a PARP ortholog affect DNA methylation in *A. immersus*, as this species may have a maintenance methylation system that is more similar to that in mammals.

3.14. The NPO aging pathway does not involve telomere-length maintenance

Some current models for regulation of aging in humans consider telomere maintenance potentially important, as somatic human cells lack telomerase activity, and thus have a finite replicative lifespan (Campisi, 2005; Verdun and Karlseder, 2007). Recently, SIRT6 has been shown to function as a telomere-specific histone H3 K9 deacetylase, which is necessary for normal telomere maintenance and for prevention of premature cellular senescence in human fibroblasts (Michishita et al., 2008). In addition to playing a role in replicative cellular aging, SIRT6 has also been shown to impact chronological aging in mice, as $SIRT6^{-/-}$ animals exhibit phenotypes characteristic of progeroid disorders (Mostoslavsky et al., 2006). We did not observe any effect on telomere length in an *npo* mutant strain. These results do not rule out the possibility, however, that mutation of *npo* might affect other aspects of telomere maintenance or stability. In fact, the aberrations seen at telomeres in *SIRT6* knockdown fibroblasts are similar to those seen in Werner syndrome cells, such as telomere deletions, duplications and fusions, with no obvious effect on the length of intact telomeres (Michishita et al., 2008). Importantly, *N. crassa* has a homolog of SIRT6, termed Neurospora Sirtuin 7 (NST-7), not found in either *S. cerevisiae* or *S. pombe* (Smith et al., 2008). It would be interesting to know whether NST-7 functions in the same aging pathway as NPO, and whether maintenance of telomere integrity is involved.

3.15. The NPO aging pathway and histone H1

The replicative aging phenotype that we observed in the *npo* mutant is novel for *N. crassa* but similar to that reported for a strain of the filamentous fungus *Ascobolus immerses* carrying a silenced epi-allele of the histone H1 (*hH1*) gene, that confers a DNA hypermethylation phenotype (Barra et al., 2000). Although *N. crassa hH1* mutants do not display hypermethylation (Folco et al., 2003), it would be interesting to know whether Neurospora *hH1* mutants show a decreased replicative lifespan, and if so, whether this involves NPO. Conversely, one could ask whether PARP inhibitors or mutation/silencing of a PARP ortholog would affect replicative aging in *A. immersus*, and if so, whether the pathway is independent of the established hH1 pathway and/or DNA methylation. Kim et al. (2004) showed that PARP-1 associates with chromatin in a manner very similar to hH1: PARP-1 increases the nucleosome repeat length and competes with hH1 in nucleosome assembly reactions. Like hH1, binding of PARP-1 to chromatin *in vitro* triggers condensation and transcriptional repression. Unlike hH1, however, PARP-1 dissociates from chromatin in the presence of NAD+, and it has been suggested that localized NAD+ levels in nuclei might control chromatin structure and transcription (Kim et al., 2004). Results of ChIP-chip experiments have shown that actively transcribed promoters have high levels of PARP-1 and low levels of hH1, and that hH1 occupancy is excluded by PARP-1 binding (Krishnakumar et al., 2008). An attractive hypothesis is that PARPs and hH1 provide related functions associated with nuclear NAD+ levels, genome stability and aging. Consistent with this possibility, dramatic loss of hH1 accompanies cellular senescence of human fibroblasts (Funayama et al., 2006). While it is intriguing that both PARP and hH1 orthologs have been implicated in replicative aging in filamentous fungi, there is currently no evidence that fungal PARPs of the PrpA class have the linker histone-like properties of PARP-1. Furthermore, they lack an amino terminal DNA-binding domain, which is required for PARP-1 chromatin association. It remains possible, however, that fungal PARPs interact with DNA binding proteins that target them to chromatin.

3.16. NPO might regulate aging in a pathway with Sirtuins

The possible function of NSTs in regulation of lifespan in *N. crassa* has not been investigated. If PARPs impact aging exclusively through indirect effects on the activity of Sirtuins, then our observation that NPO is necessary for normal replicative lifespan in *N. crassa* is difficult to reconcile with current models on how Sirtuins regulate aging in yeast and higher organisms. Current models from yeast that assume Sirtuins function exclusively to promote longevity would predict that when NAD+ is limiting, PARylation would inhibit long lifespan, because NAD+-dependent deacetylation and PARylation both consume NAD+ and produce NAM. Thus, an important question is whether localized NAD+ levels in nuclei are in fact limiting. If they are not, then NSTs and NPO could presumably act in the same or parallel pathways, with both functioning to promote longevity. Anderson et al. (2002) found that increasing the levels of NAD+ salvage pathway proteins in *S. cerevisiae* increased telomere and rDNA silencing in a Sir2-dependent manner. Although sir2 deletion mutants were not found to have elevated levels of total cellular NAD+, the authors argue that most or all of NAD+ salvage in *S. cerevisiae* occurs in nuclei, and that nuclear NAD+ salvage pathway flux is important in regulation of Sir2 deacetylase activity (Anderson et al., 2002).

Unlike Sir2, PARP-1 can dramatically reduce total cellular NAD+ levels in response to DNA damage (Zong et al., 2004). If NPO is as robust as PARP-1, and if NAD+ availability within nuclei is limiting in *N. crassa*, then NSTs and NPO may compete for NAD+, and thus function antagonistically in the same aging pathway. However, if it is also assumed that Sirtuins act exclusively to promote longevity, as some models suggest, then PARylation should have a negative affect on lifespan, and mutation of *npo* should increase longevity, which is contrary to our observations.

Please cite this article in press as: Kothe, G.O., et al. PARP is involved in replicative aging in *Neurospora crassa*. Fungal Genet. Biol. (2010), doi:10.1016/j.fgb.2009.12.012